
Article:
Zhao, M., Mills, B.J.W., Poulton, S.W. orcid.org/0000-0001-7621-189X et al. (4 more authors) (2024) Drivers of the global phosphorus cycle over geological time. Nature Reviews Earth & Environment. ISSN 2662-138X

https://doi.org/10.1038/s43017-024-00603-4

Drivers of the global phosphorus cycle over geological time

Mingyu Zhao[1,2†], Benjamin J. W. Mills[3], Simon W. Poulton[3], Bo Wan[1], Ke-Qing Xiao[4], Licheng Guo[1,2], Zhengtang Guo[1,2]

[1]State Key Laboratory of Lithospheric and Environmental Coevolution, Institute of Geology and Geophysics, Chinese Academy of Sciences, Beijing, China

[2]Key Laboratory of Cenozoic Geology and Environment, Institute of Geology and Geophysics, Chinese Academy of Sciences, Beijing 100029, China

[3]School of Earth and Environment, University of Leeds, Leeds LS2 9JT, UK

[4]State Key Lab of Urban and Regional Ecology, Research Center for Eco-Environmental Sciences, Chinese Academy of Sciences, Shuangqing Rd. 18, 10085 Beijing, China

[†]e-mail: mingyu.zhao@mail.iggcas.ac.cn

Abstract | The global phosphorus (P) cycle plays a crucial role in determining the size of Earth's biosphere, as P is a key limiting nutrient for primary productivity. There are also strong couplings between the global C, P, and O cycles through processes like photosynthesis, respiration and degradation, and thus the long-term global P cycle exerts a major influence on climate and the redox state of Earth's surface. In this review, we discuss the current understanding of the environmental forcings that control P sources from weathering and P removal through burial in marine sediments, with perspectives on avenues for future research. On land, local temperature, biota, tectonic activity, and atmospheric levels of pO_2 and pCO_2 are key forcings for P weathering. In the ocean, significant constraints on marine phosphorus burial and regeneration are imposed by factors such as organic matter flux to the sediments, ocean chemistry, redox conditions, temperature, sedimentation rate, and biological activity within the sediments. With such a large array of potential controls, further detailed study of the drivers of the global P cycle could greatly advance understanding of the operation of global biogeochemical cycles, as well as the chemical evolution of Earth's surface environment.

Introduction

Phosphorus (P) is an essential nutrient for all life, serving as a critical building block for the genetic materials DNA and RNA, the energy carrier adenosine triphosphate, and cell membranes. P is a key limiting nutrient for primary productivity in terrestrial ecosystems[1-3], and is thus widely applied as a fertilizer for agriculture production. Phosphorus is also generally thought to be the ultimate limiting nutrient for marine primary production on geologic time scales, given the high abundance of atmospheric nitrogen, which can be rendered bioavailable via nitrogen fixation[4]. The dominant P source for both modern terrestrial and marine ecosystems is P weathering on land, and marine P burial represents the main sink in the global P cycle[5].

Moreover, there are strong couplings between the global C, P, and O cycles through photosynthesis and respiration[6-8]. Therefore, the drivers of the global P cycle determine the operation of many major global biogeochemical cycles. However, current reviews predominantly focus on the operation of the global P cycle[5,9-11] rather than its environmental drivers. Substantial progress has been made on the specific aspects pertaining to the drivers of the P cycle over recent years[12-16].

Based on studies of modern soil P components, climate has been shown to have a marked impact on P weathering[17-19]. Theoretical relationships between temperature and the intensity of P weathering have also been applied to global biogeochemical models, including the use of the Arrhenius equation[20], and scaling with the weathering rates of silicates, carbonates and organic matter[8,21,22]. A quantifiable understanding of the relationship between temperature and P weathering is crucial for predicting the impacts of climate change on terrestrial and marine ecosystems, as well as agricultural production. The intensification of P weathering under

a warmer climate promotes marine productivity, which can also result in a negative feedback on atmospheric pCO_2, hence affecting the planetary thermostat. Indeed, a recent study based on a global soil data compilation has re-constrained the strength of this planetary thermostat[23].

In this review, we provide an overview of the various environmental forcings (long-term changes in background conditions) that are important for the general processes of P weathering on land and subsequent burial in the ocean, since the origin of oxygenic photosynthesis (~3.0 billion years ago). A review of the P cycle on the earlier Earth can be found elsewhere[24]. In addition to considering environmental forcings important for the modern P cycle, we also consider drivers that were likely important for the evolution of global P cycling through geological history. Finally, we offer perspectives on potential ways to further improve understanding of the drivers of both the modern and ancient global P cycle.

The main processes in global phosphorus cycle

Before discussing the drivers of the phosphorus cycle, we will first provide a brief overview of the main processes and fluxes in the global phosphorus cycle. Our focus is on the modern phosphorus cycle here, as the primary processes of the global phosphorus cycle during geologic time were likely very similar to those of the present day.

Phosphorus in bedrock is weathered and transformed into dissolved inorganic phosphorus (DIP), which is then used to produce biomass on land and in the ocean. As shown in Figure 1 and Table S1, the single major source of P to the modern ocean is riverine P generated by physical and chemical weathering on land[5], while atmospheric and volcanic sources constitute minor contributions[25]. Riverine transport of P to the ocean includes dissolved P (DIP and dissolved organic P, or DOP) and reactive particulate P[5,9,10,26]. Weathering of P on land mainly occurs through the dissolution of apatite ($25.4 \pm 5.4\times10^{10}$ mol yr^{-1}), including igneous fluorapatite (FAP: $Ca_5(PO_4)_3F$) and sedimentary carbonate fluorapatite (CFA), and the oxidation of organic matter ($1.2 \pm 0.2\times10^{10}$ mol yr^{-1}, see Supplementary Information for this estimation). Phosphorus can also substitute for silicon in igneous and metamorphic rocks, with silicate phosphorus contributing approximately 20% to the total phosphorus content of the modern crust[27]. This proportion has varied throughout Earth's history[24]. In the modern environment, approximately 55% of the phosphorus weathering flux originates from sedimentary rocks, 38% from igneous rocks and 7% from metamorphic rocks[28]. The P flux from mineral dissolution during chemical weathering is modified prior to transport by rivers, via precipitation of secondary minerals such as calcium phosphate[29] or uptake by iron and aluminium (oxyhydr)oxides in the weathering profile[30,31]. In addition, P can be removed from solution by plants and other organisms in soils[17,32,33]. The preindustrial fluxes of dissolved P and reactive particulate P from rivers to the ocean are estimated to be $2.8 \pm 0.2\times10^{10}$ mol yr^{-1} and $20 \pm 6\times10^{10}$ mol yr^{-1}, respectively (see Supplementary Text for these estimations). The dominant phases of P in suspended particles include iron-bound P, organic P and detrital apatite[34,35], although P may also be effectively transported by aluminum oxyhydroxides and clays[36-38]. A substantial amount of P can be released in a bioavailable form when riverine particles enter the ocean[5,34].

In the ocean, DOP and DIP are utilized in primary productivity[39-41]. In the oceanic interior, most P is recycled, whereby DIP is released from organic matter through respiration and can then be transported back to the surface ocean through upwelling, water mixing and/or oceanic currents, stimulating further photosynthesis[5]. Factors affecting P uptake and release in the water column include rates of primary productivity, the behaviour of the biological pump, ocean circulation (particularly upwelling), the stoichiometry of phytoplankton, oxygen concentrations and temperature[14,42,43].

As shown in Figure 1, P is dominantly delivered to sediments as organic P (P_{org}), P bound to iron (oxyhydr)oxides (P_{Fe}), or detrital P (P_{det})[12,44-47]. The latter two fluxes are sourced either directly from weathering on land or, in the case of Fe (oxyhydr)oxide-bound P, through scavenging in the water column[47-50]. Normal marine sediments are the primary sink for P, with hydrothermal processes playing a minor role (~5%)[25]. In marine sediments, reactive P (P_{reac}; representing P that is potentially bioavailable in surface and near-surface environments) burial mainly occurs in the form of P_{org}, P_{Fe} (including as vivianite; $Fe_3(PO_4)_2\cdot 8H_2O$), and

carbonate fluorapatite (CFA; $Ca_{9.54}Na_{0.33}Mg_{0.13}(PO_4)_{4.8}(CO_3)_{1.2}F_{2.48}$)[12,44,45,47]), although a considerable amount of P burial may occur in association with carbonate or opal[51-54]. Authigenic P (including CFA, carbonate P, and opal P) accounts for ~31% of P_{reac} burial on continental margins, with its contribution to deep-oceanic sediments exceeding 50% (Fig. 2 and Table S2)[5,26,55]. Organic P and P_{Fe} contribute ~32% and ~29% of the P_{reac} burial flux in continental margin settings, respectively, with lower contributions to deep-sea sediments (both ~16%, Fig. 2 and Table S2)[26,55]. Based on the size of the marine P reservoir and the total marine sinks, the residence time of P in the ocean is estimated to be in the range of 11,000-27,000 years (see Supplementary Text for this estimation). As shown in panel **c** of Figure 1 (after refs[56,57]), CFA forms in marine porewaters via the release of P from organic matter and iron (oxyhydr)oxides, a process termed diagenetic "sink-switching"[12,44,45,47]. Hydrothermal activity is a minor P sink in the modern ocean ($1.4 \pm 0.2\times10^{10}$ mol yr^{-1}), and predominantly occurs via P scavenging onto Fe-Mn (oxyhydr)oxides precipitated in hydrothermal plumes[25,58].

Phosphorus weathering

The controlling factors for apatite weathering are similar to those for silicate minerals and include temperature, biotic effects, pCO_2, and tectonic activity[19,20,59-61]. Nevertheless, the impact of these forcings on silicate and P mineral weathering can differ, due to the distinct reaction kinetics between silicate and apatite[20,62], the existence of a complex organic P cycle in the soil[17], and the significant role of particulate material in transporting reactive P to the ocean[5,34]. For instance, experimental studies have shown that the impact of land plants on P weathering can be more pronounced than on silicate weathering[33]. Therefore, P weathering may be decoupled from silicate weathering through various mechanisms, including changes in the P/Si ratio of weathering rocks[15,63], soil erosion pulses transporting reactive P to the ocean[64], the release of organic P during the collapse of the terrestrial biosphere[65], and the exposure of unconsolidated sediments for weathering during sea-level fall[26,66]. The controlling factors for the oxidation of organic matter include erosion rates, temperature and atmospheric oxygen levels[67-69]. In terms of soil P content, the controls include temperature, precipitation, biotic effects, parent rock type, slope and elevation of the weathering site, and soil organic matter content[17,19,70-72]. It is important to note that the drivers of weathering are not entirely independent and are often interrelated[28]. The influence of these forcings has been widely considered in studies of the evolution of biogeochemical cycles through Earth history[7,21,33,60].

Weathering through time (post 3.0 Ga)

The evolution of P weathering through time can be quantified based on current understanding of the influence of the various drivers. Available model results indicate a gradual increase in continental P weathering over the past 3 billion years[15]. To assess this finding, we plot a first-order estimate of the evolution of P weathering through incorporating long-term drivers such as tectonics (area, elevation, and P content of continental crust), atmospheric pCO_2, pO_2, climate, and biota (see Fig. 3 and Supplementary Information for further details). The curve of crustal P content used in this calculation is derived from reconstructing the lithological evolution of the continental crust, incorporating the measured P content of each lithological unit[15]. The shift in the areal extent of the continental crust with time is highly debated[73-76], and we have considered this uncertainty in our calculations (Fig. 3, and Fig. S1). The elevation of the continental crust has been estimated through reconstructions utilizing europium anomalies found in detrital zircons[77]. The global average temperature curve for the Phanerozoic is based on proxy records[78]. For the Precambrian, other than during the "Snowball Earth" intervals, the global average temperature was set in the range of 15-25°C, given the generally clement non-glacial environmental conditions[79]. The impact of the rise of land plants on P weathering during the Paleozoic was quantified using a previously established approach[7].

Depending on the evolution of continental area, the P weathering flux may have shown a decreasing trend from ~3.0 to 2.5 Ga due to a gradual drop in atmospheric pCO_2 during this period (Fig. 3). The weathering rate of P from the land during the "Snowball Earth" intervals in the Paleoproterozoic and the Neoproterozoic was likely substantially reduced due to the low global average temperature (<-20 to -30°C)[79]. An increase in P weathering, to 15-17% of the modern level, is indicated for the early Neoproterozoic (1-0.8 Ga), due to changes in elevation and P content of continental crust[15,77]. Lastly, the P weathering flux could have increased to >50% of the modern level during the Paleozoic (~0.43 Ga), due to the rise of land plants and an increase in crustal P content[7,15,80].

The weathering rate of P may have decreased during the Carboniferous-Permian and Cenozoic glacial intervals due to the low global average temperature (10-15°C)[78], although this effect may have been partially offset by the exposure of more shelf area for weathering due to the sea level lowlands during the glaciations[26,66]. Note that our calculations pertain solely to continental P weathering. It is important to acknowledge that seafloor P weathering could also have been substantial during the Precambrian due to the anoxic deep ocean[15,81]. Since the rate of silicate weathering must be balanced by CO_2 degassing[82,83], the total long-term (>1 million years) P weathering rate on the land and seafloor was likely dominantly regulated by degassing rates, the P content of rocks undergoing weathering, the redox state of the deep ocean, and the ratio between continental and seafloor weathering[15,81,84,85].

Tectonics

Tectonic activity is one of the major forcings for physical and chemical weathering, and it therefore plays a critical role in controlling P weathering. Tectonic activity determines rock types, their position on the moving plate surface, and the topography of the land. In particular, the area of exposed land exerts a first order control on weathering, and the growth of continental crust on a global scale has changed the exposed land area for P weathering (Fig. 3), which has been implicated as a contributing driver for the Great Oxygenation Event in the Paleoproterozoic[75]. At a regional scale, orogenesis along convergent plate boundaries or the emplacement of large igneous provinces (LIPs) within a plate can result in contrasting topography (for example, mountain chains or plateaus), which can modulate denudation rates and hence the weathering flux of P[7,19,60,86]. In particular, a notable increase in the average elevation of the continental crust may have occurred in the early Neoproterozoic (1-0.8 Ga)[77], which likely induced an increase in continental P weathering (Fig. 3), although it is important to note that other processes (discussed below) can limit the extent to which this results in higher bioavailable P concentrations in the ocean[87].

Tectonic style also influences magmatic processes and hence the P content of rocks formed in the continental crust[63,85,88]. For example, Archean magmatism was mostly bimodally distributed between tonalite–trondhjemite–granodiorite (TTG) and greenstone, both of which have low P contents. With the onset of global subduction at least since the Paleoproterozoic[89], more intermediate rocks have formed, leading to an increase in the P content of igneous rocks[63]. Moreover, the P content in igneous rocks could be influenced by the degree of melting driven by mantle cooling or the supercontinent cycle, with incompatible P enriched in the melt during lower degrees of partial melting[85,90]. Hence, a progressive rise in P concentrations in the continental crust could be driven by gradual cooling of the mantle over time[85].

It is noteworthy that mafic rocks generally contain more P than intermediate and felsic rocks (Fig. 4)[28,63,91]. In addition, basic and intermediate volcanic rocks such as basalt weather faster than acidic volcanic rocks like granite, resulting in a quicker release of P (Fig. 4)[28]. Furthermore, the P release rate from basic and intermediate igneous rocks is generally higher than from sedimentary rocks (Fig. 4)[28]. Currently, exposed magmatic rocks cover approximately 15% of the land area, contributing around 38% of the total P release rate[28]. A notable shift in the types of rocks subject to weathering has been proposed during the transition between the Neoproterozoic and the Phanerozoic (0.6-0.4 Ga), resulting in an increase in continental P weathering rates (Fig. 3)[15]. The emplacement of LIPs, primarily composed of basalts, can also enhance P fluxes due to their high weatherability and relatively high P contents, and this has commonly been implicated as a driver for increased primary productivity during the Neoproterozoic Oxygenation Event (NOE)[90] and Phanerozoic oceanic anoxic events (OAEs)[6,92]. Episodes of enhanced P supply due to the weathering of volcanic deposits may also have contributed to global climate change and carbon isotope shifts during the Late Ordovician and Carboniferous periods[93,94].

Moreover, the composition of parent rock also indirectly affects P weathering by influencing soil properties, such as soil texture, the abundance of Fe and Al (oxyhydr)oxides, clay minerals and pH[30,31,95-97]. Finally, tectonic activity also influences P weathering by affecting soil shielding, namely, the development of soil on weathering surfaces. Studies have shown that soil shielding and the aging of the land surface can substantially decrease P weathering rates[28,98]. Mountain uplift can lead to the removal of soil cover[99], consequently enhancing the transport of reactive P to the ocean via soil particulates and increasing the chemical weathering rate of P on exposed fresh rocks.

198 ***Climate***
199 The dissolution of minerals such as apatite is partly controlled by temperature[18,19,72,100]. In the simplest case,
200 the relationship between temperature and apatite weathering rate (k_A) can be represented through the Arrhenius
201 equation (Fig. 4a)[20,61,62,101]:
202
203 $$k_A = k * a_H{}^n * e^{-\frac{E_a}{RT}} * f(\Omega) \quad (1)$$
204
205 where k denotes the rate constant, a_H stands for the activity of H^+ in soil water, n is the reaction order (0.6-
206 0.9)[61,62,101], E_a is the activation energy, R is the ideal gas constant, T is the temperature in Kelvin, and $f(\Omega)$ is
207 a function of the saturation state of apatite (Ω). Through dissolution experiments, the E_a values for FAP
208 dissolution have been measured, which are in the range of 8.3-11 kcal mol^{-1} [61,101].

209 Natural systems are, however, far more complex than can be simulated through a simple equation based on
210 basic chemical principles. In particular, precipitation and runoff provide additional climatic controls on local
211 weathering rates[11,102-104]. Additionally, temperature influences the weathering rate of phosphorus by affecting
212 the viscosity of water, gas flux in the soil pile, biological activity, P sorption and desorption, and the saturation
213 state of minerals[28,104]. Precipitation and runoff can influence the leaching rate of P[105], though global data
214 compilations do not substantiate a significant overall impact of precipitation on soil P contents[23,104]. Global
215 apatite weathering rates are commonly calculated based on global runoff and temperature, often scaled with
216 silicate and carbonate weathering rates in global biogeochemical box models such as COPSE[7,21] and LOSCAR[8],
217 and through local estimates of those same factors in 'spatialized' models like SCION and GEOCLIM[106,107] (Fig.
218 4a), although a decoupling of weathering rate between different components may exist[22]. Through a
219 compilation of P contents and mean annual temperatures of global top soils, initial results from 'big data'
220 techniques for the enhancement of P weathering under warm climatic conditions have been calculated (Fig.
221 4a,c)[23]. The response of P weathering to warming in this calculation is lower than those used in the LOSCAR
222 and COPSE models, but higher than in SCION. P weathering rates increase more rapidly when the global mean
223 annual temperature is in the range of 21-23°C[23].

224 This shift in P weathering with climate provides a negative climate feedback on the timescale of millions of
225 years (Fig. 4d), as P weathering promotes primary productivity and thus the consumption of CO_2 from the
226 atmosphere[20,23]. The enhancement of P weathering under a warm climate has been invoked as a driver of
227 oceanic anoxic events during the Phanerozoic[6,23,108,109]. The acceleration of P weathering due to anthropogenic
228 climate warming poses a threat to agricultural production, lake and marine ecosystems, and fisheries[23].

229 However, it worth noting that climate can also influence P weathering through its effect on sea level over longer
230 timescales (greater than several thousand years), for example, during the ice ages of the Carboniferous-Permian
231 and Quaternary. Although the lower temperatures of glacial periods would typically reduce P weathering, this
232 effect is counteracted by increased global weathering due to the exposure of continental shelves during periods
233 of falling sea level[26,66]. On a local scale, glaciations can result in a large amount of freshly exposed silt-sized
234 sediment, with a vast surface area available for weathering. Thus, in interglacial periods in the immediate
235 aftermath of glaciation, or during glacial periods with active water flow, the sediments may be highly
236 weatherable.

237 ***Biota***
238 The evolution of continental biota had a major influence on P weathering, as organisms such as microbial mats
239 and land plants have the ability to increase P weathering rates. Microbes have great potential to increase P
240 availability and play a key role in P transformation processes[110]. Microbes can release a series of enzymes (for
241 example, phytase, C-P lyase and phosphonatase) and organic acids (for example, gluconic acid, malic acid and
242 oxalic acid) that can solubilize recalcitrant P[111]. Therefore, the rise of microbial mats during the Archean period
243 likely increased P weathering rates, although current estimates for the timing of widespread microbial mat
244 development on land have large uncertainties (from 3.8-2.3 Ga)[112]. It has been suggested that the rise of land
245 plants during the Paleozoic (~0.45 Ga) substantially increased the intensity of P weathering (Fig. 3)[7].

The enhanced strength of silicate weathering due to the rise of land plants is hypothesized to have been responsible for the drawdown of atmospheric pCO_2 and thus global cooling from the Ordovician to Carboniferous period[33,113]. Indeed, field observations indicate that vascular plants can enhance silicate weathering by a factor of 2-5[114], and it is generally believed that the rise of vascular plants substantially increased the weathering rate of nutrients such as P[33,115]. Moreover, studies on the factors that control soil P contents also support the importance of biota or vegetation for P weathering[19,72]. The organic acids secreted and the organic litter generated by land plants and microbes can reduce the pH of soils[59,116], which increases the dissolution rate of apatite (see Equation (1)), and land plants can also increase the weathering of apatite through water cycling[59]. Moreover, the roots of plants can increase the infiltration of water, thereby increasing the reaction area for weathering.

In an incubation experiment, moss was shown to amplify the P release rate from granite by ~60 times[33]. However, while this supports a marked role for plants in P weathering, other research challenges this conclusion based on the thin soil zones associated with early plants relative to the later-evolving trees[117]. Moreover, the effect of the rise of land plants on P weathering may have been episodic, due to the impact of soil age on P weathering, as effective internal cycling of P would have occurred once P in available rocks was exhausted by the first plants[2,17,32,33,72]. Despite these uncertainties, the effect of land plants on the strength of P weathering has been widely applied in global biogeochemical models[7,21,33]. While plants have the potential to enhance chemical weathering rates on land, within the Earth system, this impact would be partially mitigated by a reduction in atmospheric pCO_2[83]. On the other hand, the evolution of land plants likely increased the relative extent of continental weathering relative to seafloor weathering[84].

Atmospheric pCO_2 and pO_2

Atmospheric pCO_2 is also an important factor for P weathering, as it influences the pH of soil water[118] and thus the dissolution rate of apatite (see Equation (1)). Atmospheric pCO_2 may have been 2-4 orders of magnitude higher than modern levels during the Archean period (Fig. 3). This elevated pCO_2 would have helped to maintain considerable P weathering even though P weathering rates would have been strongly diminished by the smaller land area, lower elevation, and lower P content of the continental crust, as well as the lack of plant-enhanced weathering[7,15,77]. Overall, atmospheric pCO_2 progressively decreased from the Archean to the modern era, which negative impacted inorganic P weathering rates.

In a purely inorganic system (with no biomass on land), the activity of H^+ in soil water (α_H) is related to pCO_2 in the atmosphere[84,118]:

$$\alpha_H = K \cdot pCO_2{}^n \qquad (2)$$

where K is the equilibrium constant for carbonic acid dissociation, and n is the reaction order (~0.5). Since the reaction order of apatite dissolution with respect to α_H is 0.6-0.9 (Equation (1)), the reaction order of apatite with respect to pCO_2 will be 0.3-0.45 (Fig. 4). It should be noted that this relationship is based on the assumption that the system is strongly "fluid-buffered" (i.e., the pH of soil water is not substantially influenced by silicate weathering). However, soil water pH is also controlled by the kinetics of chemical reactions related to precipitation and evapotranspiration[118,119]. Moreover, Equations (1) and (2) may only be representative of acidic soil conditions (pH < 5), because the pH dependence of dissolution rate can be much weaker under circumneutral conditions ($5 \leq pH \leq 10$)[62,118,120], and the system becomes more "mineral-buffered" when pH > 5, which can substantially weaken the relationship between pCO_2 and soil pH. However, if we accept that chemical weathering mainly occurs in regions with heavy precipitation and low soil pH (<6), representing a "fluid-buffered" system[119], Equation (2) provides a reasonable approximation of the effect of pCO_2 on P weathering. In addition, pCO_2 may also influence weathering through its indirect effect on the growth of plants and bacteria[118].

Atmospheric pO_2 is an important factor for the oxidation of organic matter and thus the release of organic P[67,68], although weathering of organic C and P can also be decoupled due to the existence of P esters that are resistant to chemical weathering[121]. As discussed above, the contribution of organic matter oxidation to total P weathering is small (<5%), and thus the effect of pO_2 on P weathering is often neglected in biogeochemical models[22,84]. Atmospheric pO_2 may also have influenced the P flux to the ocean through an Fe-P trap in river systems during the Precambrian[122]. In this scenario, at low atmospheric pO_2 (for instance, 10% of the modern

level), the rate of Fe(II) oxidation would have been much slower, leading to the delivery of Fe(II) to rivers, where subsequent oxidation would have resulted in P scavenging by Fe (oxyhydr)oxide minerals. However, the role of rising atmospheric oxygen is complex, as higher oxygen levels would likely promote the oxidation of Fe(II) and thus retention of P in the soil profile. Lastly, atmospheric pO_2 had a negative effect on the biomass and geographic extent of land plants and thus P weathering during the Phanerozoic, due to a wildfire feedback[7].

P burial and regeneration

Since the residence time of P in the ocean is ~11-27 kyr, the P burial flux is expected to be balanced by the P weathering flux on geological timescales. While the long-term burial flux of P is ultimately affected by weathering, environmental factors can significantly impact the strength of P burial and the rate of P regeneration from sediments. The regenerative flux of dissolved P from marine sediments (as high as $90\text{-}120\times10^{10}$ mol yr^{-1})[123] significantly exceeds the input of riverine dissolved P into the ocean ($2.8 \pm 0.2\times10^{10}$ mol yr^{-1}). Consequently, the regeneration of P from sediments can profoundly impact the cycling rate and reservoir capacity of P in the ocean, thereby influencing the functioning of the marine ecosystem. For example, under euxinic seawater conditions, the regeneration rate of P can be heightened, exerting a major influence on primary productivity and the overall ecosystem[60,124].

Various factors can substantially influence marine P burial and regeneration, including the organic matter flux to the sediments (J_{org})[12,125,126], oxygen and calcium concentrations of benthic seawater ($[O_2]_{BW}$ and $[Ca]_{BW}$)[12,60,124], temperature (T)[127,128], bioturbation[47,129,130], benthic seawater pH (pH_{BW})[13], sedimentation rate[9,130], water column redox conditions[124,131-134], the stoichiometry of organic matter during photosynthesis[14,135], microbial effects on CFA burial[41,136-139], mid-ocean ridge (MOR) spreading rate[58], and the reduction of phosphate to phosphite[140]. We use a Monte Carlo-artificial neural network (MC-ANN) simulation with a published diagenetic model to help understand the relative importance of selected environmental forcings on P burial during the Phanerozoic (Box 1). This simulation suggests that the effects of J_{org}, $[O_2]_{BW}$, $[Ca]_{BW}$ and T on CFA and total P burial are more pronounced than those of bioturbation and pH_{BW}, which echoes previously published model results based on traditional sensitivity analysis[12].

Burial through time

It is challenging to estimate shifts in the P burial flux through Earth's history due to the incomplete nature of the sedimentary record and uncertainties in sedimentation rate estimates. Some data compilations suggest that the mean P content of siliciclastic marine sediments increased substantially from the latest Tonian (~800 Ma) through the Neoproterozoic (Fig. 5)[15,85,135,141]. However, it should be noted that other compilations have suggested no significant change in the median P content of Neoproterozoic to lower Paleozoic sedimentary rocks (cf. Fig. S4)[142]. Nevertheless, a possible shift in the P content of marine sediments broadly coincides with the Neoproterozoic oxygenation event and an increase in the Fe oxide content of marine shales (Fig. 5). Several explanations have been invoked for this shift in P burial, including a shift in oceanic redox state, the C:P ratio of primary producers[135], and the rise of eukaryotic organisms[141]. The covariation between P and Fe (oxyhydr)oxide contents in marine sediments supports the case that these changes could have been generated by a shift in the atmosphere-ocean redox state. Fe-bound P likely played an important role in the increased P contents of continental margin sediments. Due to the continuous diagenetic sink-switching from organic P and iron-bound P to CFA[45], the proportions of organic P and iron-bound P are lower, while the proportion of CFA is higher, in ancient marine sediments deposited in continental margin settings relative to those of modern marine sediments (Fig. 2). The proportion of detrital P is also higher in ancient marine sediments, due to the gradual decarbonation of CFA during ageing[143].

Organic flux and sedimentation rate

J_{org} influences the burial of both organic P (as it supplies organic P directly to the sediment) and CFA (Box 1). J_{org} influences CFA burial in several ways[12,47,125]. Firstly, as the driver of marine diagenesis, organic matter decomposition can substantially influence the pH of sediment porewaters[12,47], which strongly controls the saturation state of CFA. Secondly, the decomposition of organic matter releases both dissolved inorganic carbon (DIC) and DIP to porewaters, which are the main components of CFA. Finally, J_{org} can indirectly influence CFA burial through its effect on animal activity and thus the intensity of bioturbation.

Since J_{org} can influence the burial and regeneration of P in multiple ways, it is not unexpected that its effect on marine P burial is not only non-linear, but also not unidirectional (Fig. S5). This is consistent with previous findings that the relationships between environmental forcings and marine P burial are usually non-linear[12,47,130]. A decrease in P burial efficiency coupled with an increase in productivity and organic P export to sediments over a timescale of several thousand years has been observed in Arabian Sea sediments[126], suggesting that the export of organic P does not necessarily ensure the burial of CFA in marine sediments. This is also supported by our model simulation (Fig. S5). J_{org} may have risen in tandem with the proposed enhancement of the biological pump during the Neoproterozoic[144]. However, the specific impact of J_{org} on P burial during this event is yet to be explored.

It has long been understood that sedimentation rate exerts a strong control on marine organic matter preservation and thus P burial[145-147]. Observations show that marine P accumulation rate has a strong positive correlation with sedimentation rate (Fig. 6)[9,148], which is also supported by model simulations[130]. The positive relationship between sedimentation rate and total marine P burial may partially reflect higher delivery rates of reactive Fe phases to the seafloor under higher sedimentation rates, including Fe-bound P. Reactive Fe phases fuel iron reduction and associated increases in pH (buffering porewaters against pH decreases associated with aerobic organic matter remineralization, sulfate reduction-associated deprotonation, and pyrite oxidation), fostering increased rates of CFA formation. Similarly, higher delivery rates of Fe-bound P under higher sedimentation rates would provide more P for incorporation into CFA during diagenetic sink-switching. Moreover, the transfer of organic P to the subsurface of sediments is also enhanced under higher sedimentation rates[130]. The slope of P/sediment accumulation rates is approximately 1.0, reflecting the combined effects of reactive particulate P carried by detrital particles and the dilution effect of faster sediment accumulation on P burial[148]. Due to difficulties in estimating sedimentation rate in ancient sediments, the role of sedimentation rate on P burial and regeneration through Earth's history remains to be explored in detail.

Temperature

It has been suggested that elevated temperatures may lower the saturation state of CFA, consequently diminishing CFA formation[13]. Yet, a comprehensive diagenetic model indicates that temperature can enhance CFA formation in marine sediments, owing to its positive impact on the reaction rate constant[127]. Temperature can influence marine P burial and regeneration in multiple ways[127], including modifying reaction rates, solubility (K*sp*), activity coefficients, diffusion coefficients, dissociation constants, seawater pH, seawater dissolved oxygen concentrations, bioturbation, sedimentation rates, and primary productivity (via organic matter loading to sediments).

The substantial influence of temperature on both organic P and CFA burial (Box 1) occurs because temperature substantially affects the rates of CFA formation and P release through organic matter decomposition[127]. The activation energy for organic matter decomposition in coastal sediments is in the range of 25 to 130 kJ mol^{-1} [149-152]. Therefore, higher temperatures promote the decomposition of organic matter, resulting in less organic P burial and more phosphate release into pore waters for CFA formation. The activation energy for CFA precipitation is ~47 kJ mol^{-1} [128]. This indicates that the direct effect of elevated temperature is a substantial acceleration of CFA formation, although this relationship could become more complicated if substantial ocean anoxia develops under climate warming[127]. These model results are consistent with observed increases in phosphorite burial during the last interglacial period, both in the Arabian Sea and along the Peru margin[153-157].

High temperatures will therefore likely promote P burial over geological timescales, as accelerated P burial is required to balance the enhanced P weathering expected in a warmer climate[8,20,61]. The increase in P burial and reduction in P regeneration under a warm climate may, to some extent, counterbalance the impact of heightened P weathering, although the influence of oceanic anoxia on P regeneration might be more pronounced under warmer climatic conditions[127].

Ocean chemistry

Seawater calcium and fluorine concentrations, as well as pH, can also have notable influences on P burial and regeneration. Calcium is the most abundant element in CFA ($Ca_{9.54}Na_{0.33}Mg_{0.13}(PO_4)_{4.8}(CO_3)_{1.2}F_{2.48}$)[158], and

seawater Ca is the most important source of Ca for CFA formation in the upper sediment profile. Therefore, seawater Ca concentrations have a substantial influence on the saturation state and, thus, the precipitation rate, of CFA (Box 1)[12]. Given the large variations in seawater Ca concentrations (~8-30 mM) throughout the Phanerozoic[159-161], seawater Ca concentration is likely to have had an important influence on the evolution of the P cycle and thus atmospheric oxygenation over timescales greater than 1 Myrs (according to the residence time of seawater calcium)[12]. This is supported by a compilation of P phase partitioning data for deep-sea sediments during the Cenozoic, which shows a gradual decrease in the proportion of reactive P buried as CFA, in parallel with a contemporaneous decrease in seawater Ca concentrations (Fig. 6)[12]. More data on both seawater Ca concentrations and P species are required to evaluate the role of seawater Ca on CFA burial prior to the Cenozoic.

Further evidence for the influence of Ca on CFA burial arises from an observed change in the relative proportions of Ca-P and Fe-P in sediments across salinity gradients (Fig. 6)[162,163], which has been used as a proxy for paleosalinity. Since the Ca concentration of modern normal seawater (~10 mM) is much higher than that of river water (~0.6 mM), the salinity gradients can be translated into Ca concentration gradients (Fig. 6). The increase in the proportion of Ca-P with elevated salinity and Ca concentration results from the interaction between sediments and dissolved seawater Ca[162,163], most likely via the formation of CFA. Since fluorine is a major component of CFA, the evolution of seawater F may also exert a marked control on marine P burial rates.

It has been suggested that a decrease in seawater pH during OAEs might substantially reduce the formation rate of CFA, consequently increasing the P regeneration rate[13]. However, analyses using the SEDCHEM diagenetic model do not support a major role for seawater pH in CFA formation in typical marine sediment (Box 1)[12]. It is known that porewater pH substantially influences the saturation state and thus the burial rate of CFA, as it affects the dissociation of both carbonate and phosphate ions. However, porewater pH is controlled not only by seawater pH, but also by multiple chemical reactions and adsorption processes occurring within the sediments. Therefore, seawater pH may not necessarily have a substantial influence on CFA and thus marine P burial if the layers where CFA forms are not close to the sediment-seawater interface[12]. This is supported by the phase partitioning of P in deep-sea sediments during the Paleocene-Eocene thermal maximum (PETM)[164]. Marine pH and the amount of $CaCO_3$ in deep-sea sediments dropped substantially during the PETM, but the amount of CFA increased[164]. This is expected, as "sink-switching" from iron-bound and organic P to CFA in deep-sea sediments is slow and likely occurs at depth in the sediment pile[55]. That being said, there are sites where CFA formation can be very close to the sediment-seawater interface (<5 cm), such as during the slow formation of phosphorite in sediments of upwelling regions[156,165,166]. Seawater pH may thus have a substantial influence on CFA burial in such settings. Therefore, the lack of phosphorite during the Archean and its low occurrence frequency during the Proterozoic (Fig. 5)[141] could be relate to high atmospheric pCO_2 and low pH during these periods[167].

Redox state

The oceanic redox state (i.e., oxic, dysoxic, euxinic or ferruginous) exerts a strong influence on P burial on both short and long timescales (from several kyrs to >1 Myrs). It has long been known that ocean euxinia (anoxic and sulfide-rich conditions) enhances organic P regeneration from sediments[124,168-171]. The total molar organic C/organic P burial ratio (C_{org}/P_{org}) is ~170 in modern oxic continental margin settings, but is much higher (~470) under modern euxinic to suboxic oceanic conditions (Fig. 2, and see Tables S2 for the compilation). Similarly, the molar total organic C/total P burial ratio (C_{org}/P_{total}) in modern euxinic to suboxic settings (~133) is also higher than that in oxic settings (~63) (Fig. 2, Table S2). The average C_{org}/P_{org} value for oxic environments on the continental margin (~170) is slightly higher than that of the deep ocean (~104) (Fig. 2, Tables S2), due to the admixture of organic matter from plants in continental margin sediments[172]. A correlation has been identified between the molar C_{org}/P_{total} ratio in modern marine sediments and the concentrations of H_2S and O_2 in the water column through a data compilation (Fig. 2, Table S2)[171]. C_{org}/P_{org} ratios are also higher in ancient marine sediments due to the gradual sink-switching from organic P to apatite[45], with average values of 440, 2970 and 2930 for oxic, ferruginous and euxinic settings, respectively (Fig. 2, Table S3). Although C_{org}/P_{org} ratios are similar between euxinic and ferruginous settings, C_{org}/P_{total} ratios are commonly lower in ferruginous settings, likely due to the enhanced ability of many ferruginous settings to trap the P released during remineralization of organic matter (for example, via formation of vivianite or re-

adsorption to Fe (oxyhydr)oxides close to the sediment-water interface[45,132,176]). The enhancement of P release back to the water column can further boost primary productivity and the spread of anoxia/euxinia, resulting in a positive productivity feedback. This theory has been widely incorporated into biogeochemical models[129,168,173-175] and has been used extensively to explain the evolution of oceanic redox state in the geological past[144,171,176-178].

The bacterial decomposition of organic matter tends to selectively break down phosphorus-rich compounds, such as proteins and nucleic acids, resulting in an enrichment of P-poor carbohydrates in the organic residue[171,179]. In oxic environments, a greater amount of regenerated phosphate tends to be sequestered in sediments, trapped by iron (oxyhydr)oxides or stored as intracellular polyphosphate granules by microbes[124,137,171]. These factors contribute to the lower C_{org}/P_{total} ratios in oxic marine sediments[124,171]. Moreover, the marine oxygen level can also influence the burial of CFA (Box 1)[12,125,130]. Model results show that elevated oxygen levels generally promote the formation of CFA[12,130]. This is mainly due to the effect of oxygen on the stabilization of Fe-(oxyhydr)oxides, to which P can be adsorbed and buried to deeper depths in the sediment, before "sink switching" from Fe-bound P to CFA (Fig. S6). Conversely, low CFA formation rates during OAEs may also be attributed to the effect of oxygen on CFA formation, although low CFA formation rates have also been interpreted as a reflection of low pH and generally higher temperatures[13].

Ferruginous conditions are commonly considered to have dominated the deep ocean during the Precambrian and early Paleozoic[180,181]. The possible substantial increase in the P content of siliciclastic sediments during the latest Tonian and through the Neoproterozoic (Fig. 5)[141] may be due to an enhanced source of P coupled with P removal from the ocean under ferruginous conditions, via the formation of Fe(II)-P minerals such as vivianite[133], coprecipitation with green rust[182] and/or scavenging by Fe(III) minerals[131,132]. However, some works doubt the effect of Fe(III) (oxyhydr)oxides in scavenging P, due to high silicon content in the Precambrian ocean[183]. Efficient P removal under ferruginous conditions is supported by low organic carbon to reactive P ratios (with a mean value of 65, Fig. 2 and Table S3) in ancient sediments, suggesting that ferruginous conditions have the potential to enhance P removal to the sediments, although this is not always the case[184]. This contrasts with the substantial increase in P regeneration observed under euxinic conditions[124,169,170,185]. The high C_{org}/P_{org} ratio and low proportions of iron-bound P and organic P in ferruginous sediments (Fig. 2) could be due to enhanced sink switching of P from iron oxides and organic matter to apatite. The C_{org}/P_{total} ratio in ferruginous sediments is lower than that in euxinic sediments but higher than in oxic sediments (see Fig. 2). This indicates that the P regeneration rate in ferruginous sediments falls between the rates observed in oxic and euxinic sediments. While the formation of Fe-P minerals such as vivianite is supported by observations from modern ferruginous P-rich lakes[186,187], this pathway has been challenged by investigations of ferruginous Mesoproterozoic sediments[188], which shows the possible formation of Fe(II)-silicate phases and CFA, rather than Fe(II)-P minerals, under the likely $SiO_{2(aq)}$-rich settings of the Precambrian. Indeed, the concentration of water column phosphate can exert a strong control on the pathway for P deposition under ferruginous conditions, with high phosphate concentrations promoting vivianite formation, whereas lower oceanic concentrations favour P drawdown in association with green rust[134].

Bioturbation and other biological activity

Bioturbation can induce sediment mixing and non-local chemical exchange between porewater and seawater, and thus plays an important role in global biogeochemical cycles. The rise of bioturbation began in the early Cambrian, and it has been suggested that even the limited extent of bioturbation at this time could have substantially enhanced global marine P burial, thereby further deoxygenating the ocean-atmosphere system[47,129,144,189,190]. However, other models suggest that biodiffusion and bioirrigation may have opposite effects on marine P burial[130,191]. The mixing of sediments by biodiffusion can increase marine P burial by transporting solid P phases deeper into the sediment pile, which decreases the P efflux from the sediments to seawater[130]. However, bioirrigation (non-local exchange of solutes between porewater and seawater) can promote P recycling rather than burial[130]. Therefore, the overall effect of bioturbation on marine P burial depends on the relative intensity of biodiffusion versus bioirrigation.

Although there have been substantial advances in simulating the effect of bioturbation on marine P burial, current parameterizations of bioturbation are likely still over-simplified[130]. The biodiffusion term used in

current P burial models[12,47,130] represents a local process that mixes sediment between adjacent layers. However, most types of sediment transport by animals, such as conveyor-belt feeding and reverse conveyor-belt feeding, are non-local processes that transport sediments between non-adjacent layers[47,192]. The bioirrigation term used in current P burial models is a one-dimensional simplification of a complex three-dimensional process [12,47,130,193,194], and more accurate future representations may shed new light on the modification of global biogeochemistry by bioturbating organisms. It is also worth noting that oxygen availability and bioturbation are not fully independent forcings influencing P burial[130].

Microbes can also play an important role in P burial. Numerous bacteria in anoxic sedimentary environments, such as sulfide-oxidizing bacteria *Beggiatoa and Thiomargarita,* and magnetotactic bacteria of the *Magnetococcaceae* family, have the ability to store polyphosphate in their cells[137,195,196]. A marked role for microbes in the formation of diagenetic apatite has long been invoked[41,136-139], which may weaken the modelled relationships between environmental forcings and CFA burial based solely on inorganic chemistry. A close correlation between concentrations of apatite and the abundance of the giant sulfur bacterium *Thiomargarita namibiensis* has been observed in sediments of the Namibian shelf[137]. The important role of *Thiomargarita namibiensis* in apatite formation is further supported by incubation experiments[138]. The episodic breakdown of polyphosphate and release of P to anoxic porewaters by polyphosphate-accumulating bacteria may be the reason for the formation of diagenetic apatite in upwelling regions[137]. Moreover, grains of polyphosphate generated by diatoms and cyanobacteria could act as the mineral nucleus for the precipitation of diagenetic apatite in non-upwelling regions[41]. Microbial processes have also been invoked to explain the origin of phosphorite ~2 billion years ago[139].

Lastly, biological innovations such as the rise of eukaryotes during the Proterozoic, and zooplankton during the early Cambrian, have been suggested to impact marine P burial through their effects on the biological pump[144,197]. The enhancement of the biological pump may have decreased the diagenetic regeneration of P[144]. This is attributed to the augmented efficiency of the biological pump, which would result in a reduction in oxygen consumption within the water column. Consequently, this may have contributed to an elevation in the oxygen levels of deeper seawater. Under oxic seawater conditions, there is a diminished regeneration of P[60,124]. However, other biogeochemical models suggest that the influence of eukaryotes and zooplankton on the biological pump was minor[198].

Other forcings

The stoichiometry (i.e., the C:P ratio) of organic matter produced from photosynthesis may have a substantial effect on global P burial[14]. The average C:P ratio for organic matter in the modern ocean is the aforementioned "Redfield ratio" of 106:1[199]. However, substantial spatial variation in C_{org}/P_{org} occurs in the modern ocean, due partially to variability in the phytoplankton community composition[200,201]. In particular, the C:P ratio of eukaryotes is on average lower than that of prokaryotes[42], which may have contributed to the shift in sedimentary P contents during the Neoproterozoic[141]. Marine C:P ratios also vary with environmental forcings such as oceanic redox state, temperature and local P concentrations in seawater[201-205]. Based on a biogeochemical model, it has been proposed that the C:P ratio of planktonic organic matter decreased throughout the Phanerozoic due to changes in global average temperature and marine P availability[14].

MOR spreading rate influences the flux of Fe(II) to the ocean and thus the formation rate of iron-manganese (oxyhydr)oxides in the water column. Since P scavenging associated with iron-manganese (oxyhydr)oxides formed in hydrothermal plumes has been estimated to represent ~5% of modern marine P burial[25,58], a change in MOR spreading rate over time likely influenced global marine P burial rates. It is also possible that the related anoxic weathering of basalt on the ocean floor was a substantial source of P on early Earth[81].

Summary and future perspectives

Studies of both modern soils and the ancient P cycle indicate that P weathering on land is primarily controlled by tectonics, biota, temperature and pCO_2. Phosphorus burial and regeneration are influenced by various

environmental factors, including the organic matter flux to sediments, ocean chemistry and redox conditions, temperature, sedimentation rate, and biological activity in marine sediments. Changes in these factors and their impact on P weathering and regeneration have likely substantially shaped the evolution of the carbon and oxygen cycles, climate, and the biosphere over deep time.

Although there have been substantial advances in understanding P weathering, a quantitative understanding of some of the relationships between various environmental forcings and P weathering remains limited. For instance, the biota on land evolved from microbial mats and lichens to non-vascular plants, and eventually to vascular plants, including seed-producing gymnosperms and flowering angiosperms. However, quantitative relationships between different land biotas and continental P weathering remain highly debated[33,114,117,206,207], and it is uncertain to what extent the quantitative results of laboratory simulations can be applied to natural systems. Moreover, the relationships applied between environmental forcings and P weathering were often based on simple chemical principles and did not account for the complex interrelations between these forcings. For example, earlier estimates of the effect of pCO_2 on P weathering were often derived from basic chemical principles of mineral dissolution and straightforward relationships between pCO_2 and soil pH. However, soil pH is also influenced by silicate weathering and is affected by precipitation and numerous other factors[119]. Furthermore, chemical weathering is not limited to mineral dissolution[208].

Our limited understanding of the spatio-temporal evolution of environmental forcings hinders precise estimates of the evolution of P weathering. For example, tectonic activity can influence P weathering through its effect on elevation and the types of parent rocks available for weathering[15]. We can, however, only roughly constrain the evolution of tectonic activity (including the evolution of topography and lithology) through time, especially during the Precambrian. Often, the effect of tectonics on P weathering has been simplified to a single linear "uplift" coefficient in global biogeochemical modelling[7,21,60], which is insufficient to accurately capture the full impact of tectonic activity on P weathering. In more recent studies, calibrated catchment-scale weathering models[102,103], laboratory simulations of chemical weathering, and big data analyses of environmental factors, including soil and river chemistry, have been used to advance understanding of the influence of pCO_2, biota, climate and tectonics on P weathering. Following these insights, more recent global biogeochemical models are moving towards spatially-resolved representations of climate, tectonics and weathering[106,107,209].

Looking ahead, machine learning methods hold substantial potential for improving the accuracy of predicting phosphorus weathering based on environmental variables. More precise data on environmental factors, such as the evolution of plants, lithology, topography, temperature, and continental runoff, will undoubtedly aid in evaluating the history of phosphorus weathering on land. Additionally, given that seafloor weathering may have been substantial during the Precambrian, it is crucial to deepen our understanding of phosphorus behavior during anoxic seafloor weathering.

Biogeochemical models have been extensively used to study the controlling factors for marine P burial. However, since conditions can vary significantly between different marine sites, this might strongly limit the transferability of model results. Moving forward, additional empirical data on phosphorus burial in various depositional settings can be used to calibrate diagenetic models, thereby improving their transferability. These data can also be valuable for analytical methods that require big databases, such as machine learning. Laboratory incubation experiments using marine sediments[138] are likely a promising way to understand the influence of environmental factors on phosphorus burial. A deeper mechanical understanding of phosphorus diagenetic pathways can still be achieved through measurements of sediments and pore water in various depositional settings, using advanced techniques such as X-ray absorption near-edge spectroscopy[210] and atomic probe tomography. Moreover, additional data on environmental forcings and the burial of various phosphorus species throughout Earth's history will undoubtedly aid in evaluating the impact of different environmental drivers on phosphorus burial.

Glossary

ARTIFICIAL NEURAL NETWORK

A subset of machine learning algorithms. Its name and structure are inspired by the human brain, as it mimics the way of signal transfer between biological neurons.

ULTIMATE LIMITING NUTRIENT

The most important nutrient that determines the production rate of new organic matter by phytoplankton or plants.

NEGATIVE FEEDBACK

A process that diminishes the initial effects.

PLANETARY THERMOSTAT

A process that can stabilize the climate of a planetary.

GREAT OXYGENATION EVENT

Earth's first major rise in atmospheric oxygen, which occurred between 2.4-2.1 billion years ago.

PLATE TECTONICS

A theory that Earth's lithosphere is divided into a number of large tectonic plates.

ACTIVATION ENERGY

The minimum amount of energy required to begin a chemical reaction.

MICROBIAL MAT

A multi-layered sheet of microorganisms.

FIRE FEEDBACK

Fires burn more intensely under increased atmospheric oxygen, which will consume oxygen and stabilize the atmospheric oxygen level.

PHOSPHORUS REGENERATION

Release of phosphorus back into seawater through the diagenetic liberation of phosphate from marine sediments.

MONTE CARLO

A mathematical technique that predicts the probability of a range of outcomes when random variables are present.

FERRUGINOUS

Anoxic and iron-rich conditions in water column.

BIOTURBATION

The physical movement of solids and solutes in sediments by fauna.

PHOSPHORITE

A P-rich sedimentary rock consisting of carbonate fluorapatite or francolite.

REACTIVE PHOSPHORUS

A combination of adsorbed phosphorus, organic phosphorus, iron-bound phosphorus and authigenic phosphorus phases in sediments.

SINK-SWITCHING

The transformation of one chemical phase of a component (for example, P) to another during diagenesis in sediments.

EUXINIC
Anoxic and sulfidic conditions in the water column.

POSITIVE FEEDBACK
A process that amplifies the initial effects.

GREEN RUST
A mixed ferrous-ferric phase that may have been an important precursor mineral during deposition of banded iron formations.

REDFIELD RATIO
The average atomic ratio of carbon, nitrogen and phosphorus in marine phytoplankton.

NON-LOCAL CHEMICAL EXCHANGE
Chemical exchange between non-adjacent sediment layers.

BIODIFFUSION
The mixing of solids and solutes in sediments by fauna.

BIOIRRIGATION
The exchange of solutes between porewater and seawater through the borrowing of fauna.

CONVEYOR-BELT FEEDING
Transfer of particles from depth within sediments to the sediment-water interface by fauna.

BIOLOGICAL PUMP
The fixation of inorganic carbon to organic carbon in the surface ocean and transport to the deep ocean.

Figure Captions

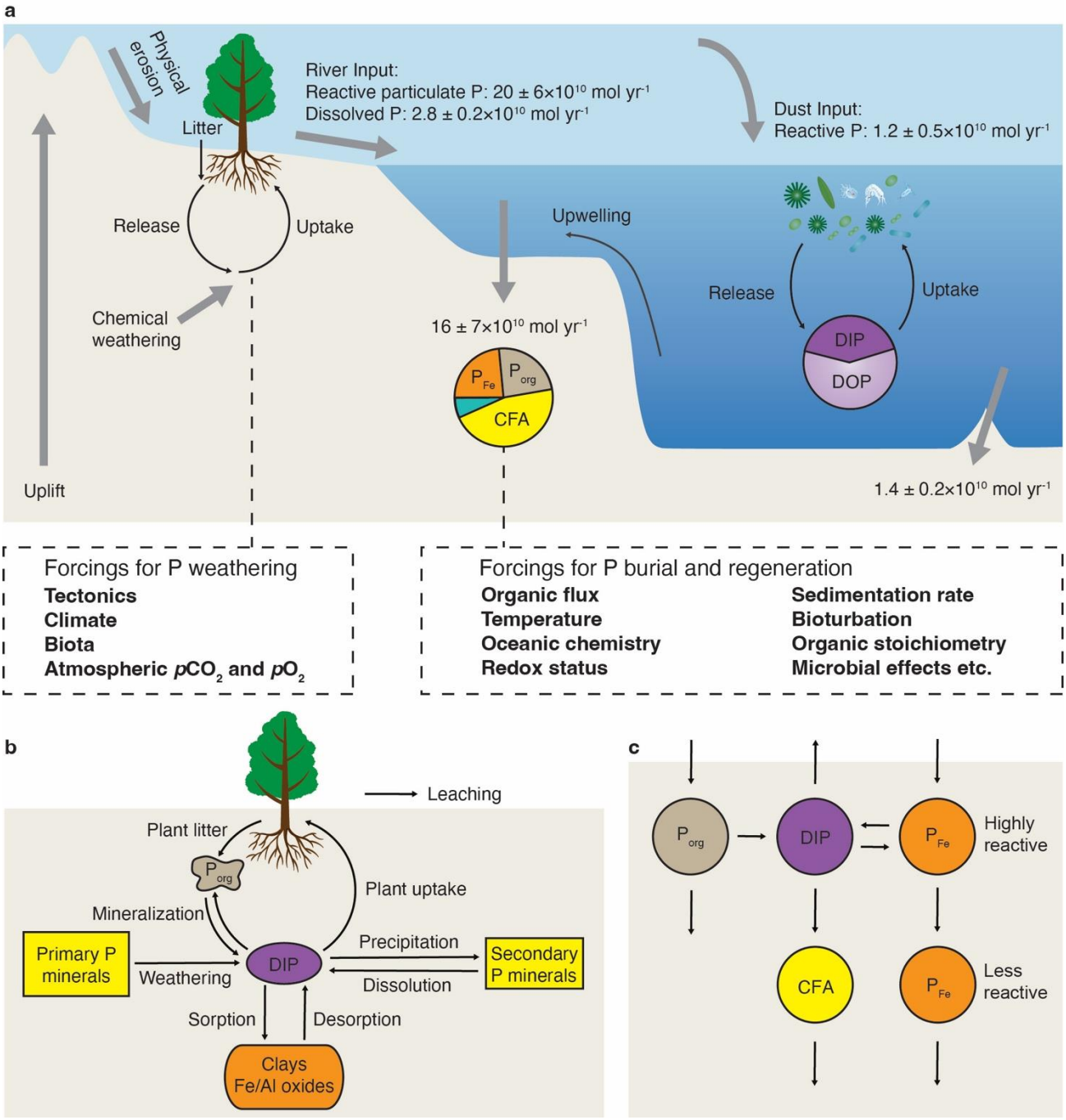

Figure 1. **Schematic diagram of the global P cycle. a |** Schematic diagram and environmental forcings for the global P cycle. Flux values pertain to the pre-industrial period. See the Supplementary Information for detailed estimates of these fluxes. The forcings for P weathering and burial are shown in the dashed boxes. **b |** Schematic diagram of P weathering processes. **c |** The main pathways for P burial in marine sediments. CFA, carbonate fluorapatite; P_{org}, organic P; P_{Fe}, P bound to iron (oxyhydr)oxides; DIP, dissolved inorganic phosphorus; DOP, dissolved organic P.

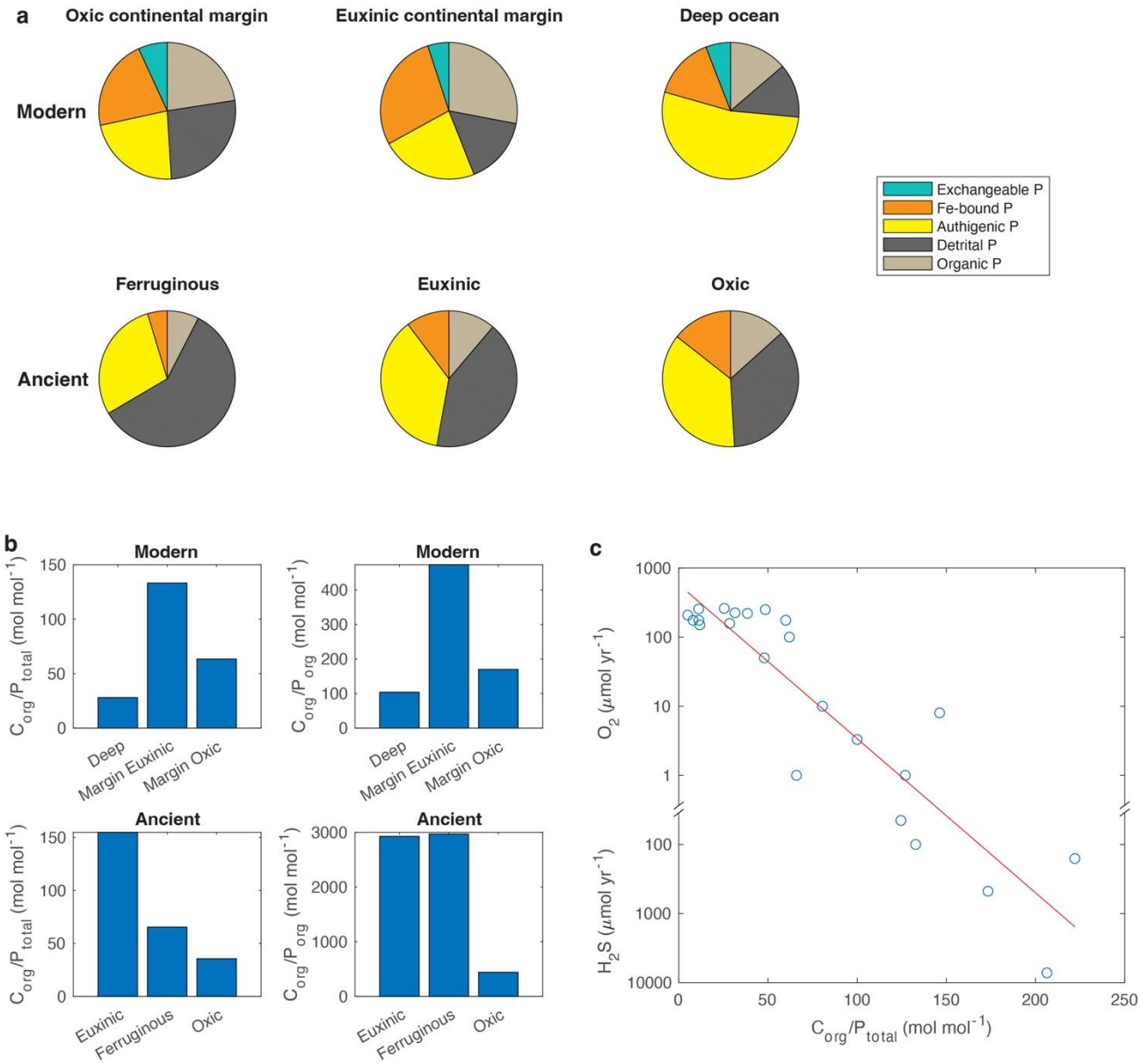

Figure 2. **Speciation of P burial, C_{org}/P_{total} and C_{org}/P_{org} in different marine environments. a |** Speciation of P burial in both modern and ancient environments. **b |** C_{org}/P_{total} and C_{org}/P_{org} of siliciclastic sediments in modern and ancient environments. Authigenic P is the sum of CFA, carbonate P and opal P. See Tables S2 and S3 for the compiled data. The ancient sediment data are from continental margins, as pre-Mesozoic deep-sea sediments were largely subducted. **c |** Relationship between mean C_{org}/P_{total} and mean O_2 and H_2S concentrations in modern marine sites. The data are mainly sourced from Ref[171] (see Table S2 for the complied data).

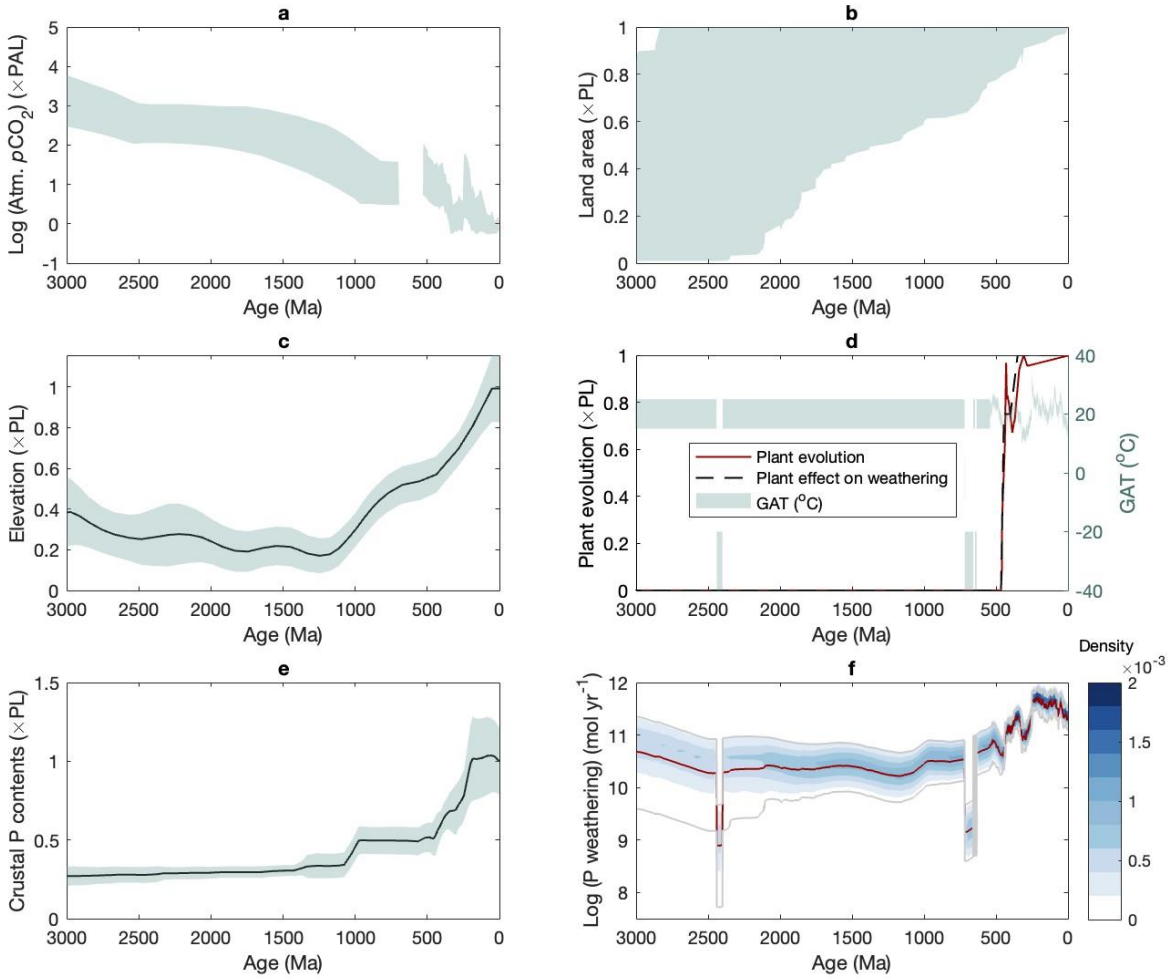

Figure 3. **Calculation of the evolution of continental P weathering.** Panels **a-e** show the parameters used in the model. **a |** atmospheric pCO_2. The Precambrian trend is from ref[211], and the Phanerozoic trend is from ref[212]. **b |** Land area. The ranges of variation are based on refs[73-76], and see Supplementary Figure 1 for the plots of each curve showing the evolution of land area. **c |** Elevation of the continental crust[77]. **d |** Plant evolution (red)[80], plant effect on weathering (black)[7] and global average temperature (GAT) (shadow)[78,79]. The shadow represents the 95% confidence interval. **e |** P contents of average weatherable crust[15]. The shadow represents the standard error. **f |** Calculated results of P weathering. The density of the shadow is linearly correlated with probability. The red line represents the mean values, and 95% of the results fall within the range marked by the grey lines. See Supplementary Information for a detailed description of this calculation. PAL, present atmospheric level; PL, present level.

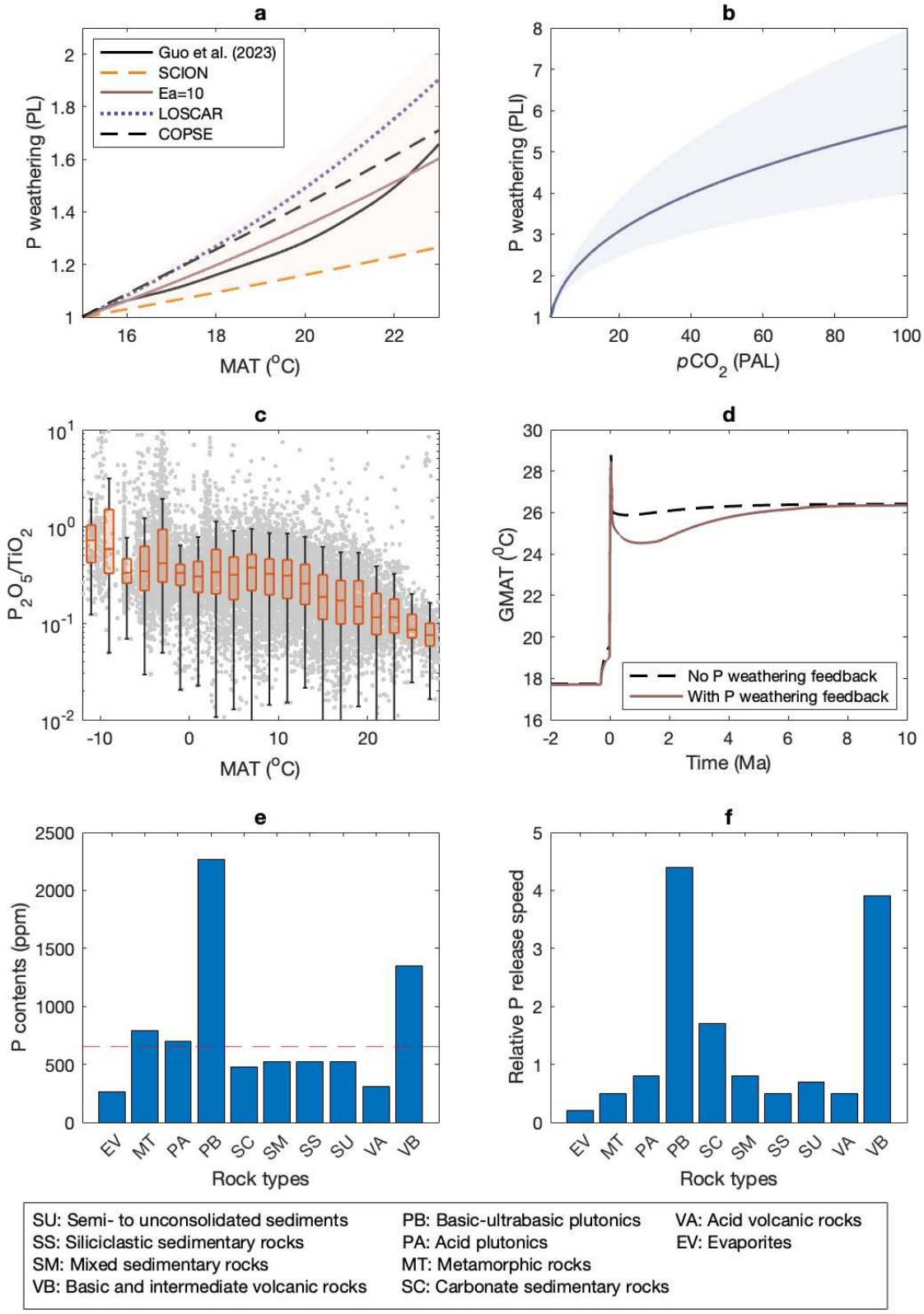

Figure 4. **The effects of temperature, pCO_2 and rock types on P weathering. a |** The relationship between P weathering and global mean annual temperature used in global biogeochemical models. PL represents the present level of P weathering at a global mean annual temperature of 15°C. The line for Ea = 10 kcal mol^{-1} is calculated using the Arrhenius equation[20]. The pink shadow represents an E_a range of 5-15 kcal mol^{-1}. The

relationships for COPSE, LOSCAR and SCION are calculated using the model versions in ref[8,21,106]. **b |** The relationship between P weathering and pCO_2. This calculation includes only the inorganic effect of pCO_2 on P weathering (see text for details). The shadow represents reaction orders in the range of 0.3-0.45. The line represents a reaction order of 0.375. **c |** The relationship between P_2O_5/TiO_2 and mean annual temperature (MAT) for global topsoils (data from ref[23]). The dots are the original data. Also shown is the box chart, presenting the median, upper quartile, lower quartile, and whiskers. **d |** The effect of the P weathering feedback on climate during the Permian-Triassic mass extinction event[23]. **e |** Average P contents in rocks on modern continents[28]. The dashed line represents the average P content of the continental crust[213]. **f |** Ratio of total P release (%) to total area (%)[28]. PAL, present atmospheric level; PL, present level; PLI, present P weathering due to inorganic processes; GMAT, global mean annual temperature.

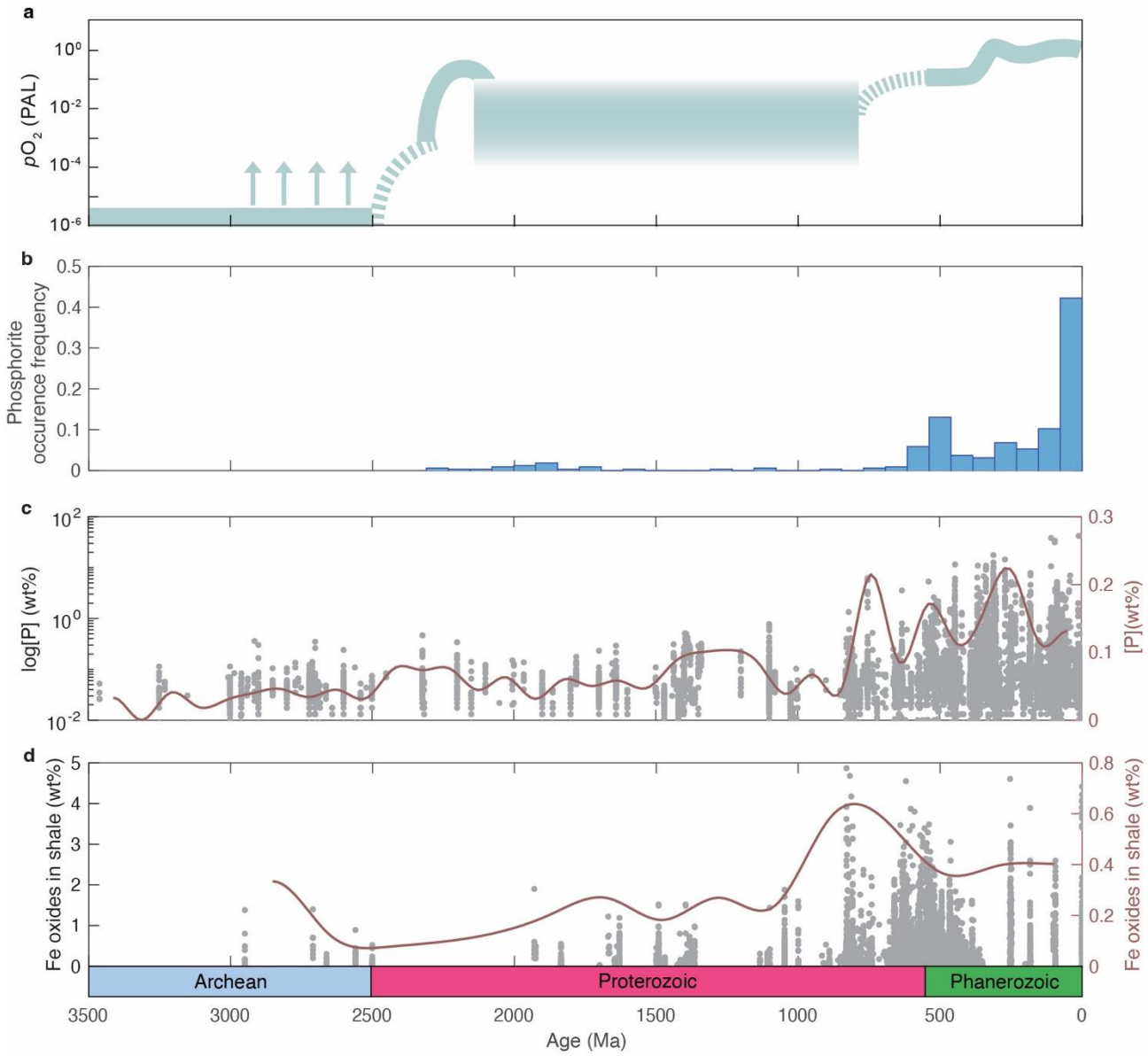

Figure 5. **Evolution of P burial through time. a |** Evolution of atmospheric pO_2, modified from ref[214]. Arrows represent potential "whiffs" of oxygen in the late Archean. **b |** Occurrence frequency of phosphorite through time (normalized to the total count)[141]. **c |** Evolution of the P content of siliciclastic marine sediments through time, with the line representing the average values of 100-million-year bins. **d |** Evolution of the Fe (oxyhydr)oxide content of marine shale through time, with the line representing the average values of 200-million-year bins. Data for P is shown in Table S4 (mainly from ref[141]), and data for Fe (oxyhydr)oxides is

from ref[22,215]. Note that the data points and lines in panels **c** and **d** are plotted on different y-scales. PAL, present atmospheric level.

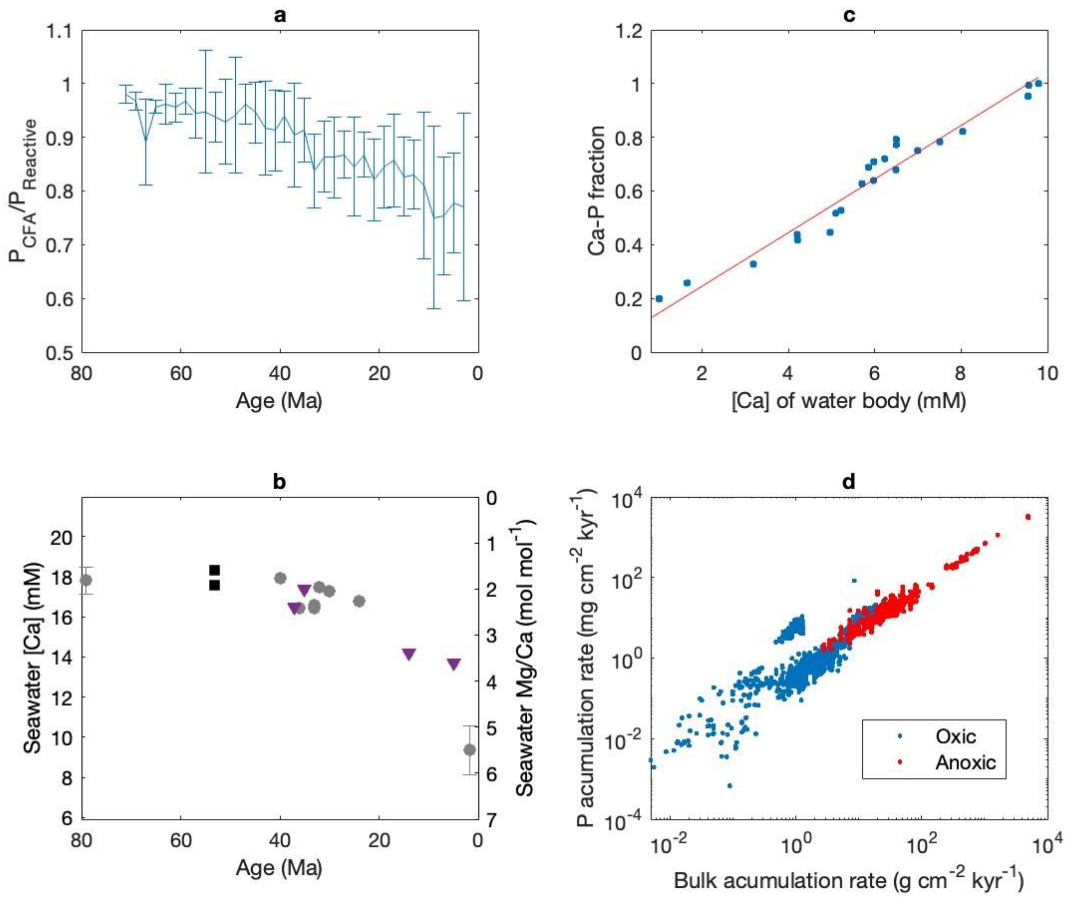

Figure 6. **Evidence for the influence of seawater calcium concentration and sedimentation rate on P burial. a |** Variation in the proportion of carbonate fluorapatite (CFA) burial (relative to total reactive P) in deep-sea sediments during the Cenozoic. See ref[12] for the data compilation. Points are the mean values of 2 Myr bins, and the error bars represent one standard deviation (1σ). Black line represents the model output of ref[12]. **b |** Seawater Ca concentration records during the Cenozoic[159-161]. **c |** Relationship between the Ca-P fraction in modern sediments and Ca concentrations in bottom waters. Data for Ca-P fraction and salinity are from ref[162]. The Ca-P fraction is relative to the sum of Ca-P and Fe-P. The Ca concentration of the water body is calculated using the salinity, with assumptions on the Ca concentrations of freshwater (0.6 mM) and seawater (10 mM). The red line shows the result of the linear fit. **d |** Relationship between the bulk accumulation rate of sediments and the P accumulation rate in both oxic and anoxic marine settings[148].

Box 1 **| Relative importance of environmental forcings for marine P burial**

To better understand the relative importance of the different environmental forcings on marine P burial in the Phanerozoic, we performed a Monte Carlo (MC) simulation using a diagenetic model (see Supplementary Text and Supplementary Tables 5-7 for a detailed description of this model). In this simulation, we varied key parameters within their likely Phanerozoic ranges. We then applied an artificial neural network (ANN; see Fig.

S2 for the flow chart of this method) to disentangle the complex relationships between different processes (see the figure in the Box and Fig. S3). The diagenetic model is modified from REF[127], with the removal of the temperature responses of bioturbation, bottom seawater pH, bottom seawater oxygen level, and organic matter flux to sediments, as these processes are treated as independent drivers of P burial in the current analysis.

This simulation suggests that the organic matter flux to sediments (J_{org}), oxygen and calcium concentrations of benthic seawater ($[O_2]_{BW}$ and $[Ca]_{BW}$), temperature (T), bioturbation, and benthic seawater pH (pH_{BW}) all exert an important influence on CFA burial, consistent with previous findings through model sensitivity analyses[12,127,130]. Our simulations also suggest that $[O_2]_{BW}$, T, bioturbation and J_{org} are important for organic P burial.

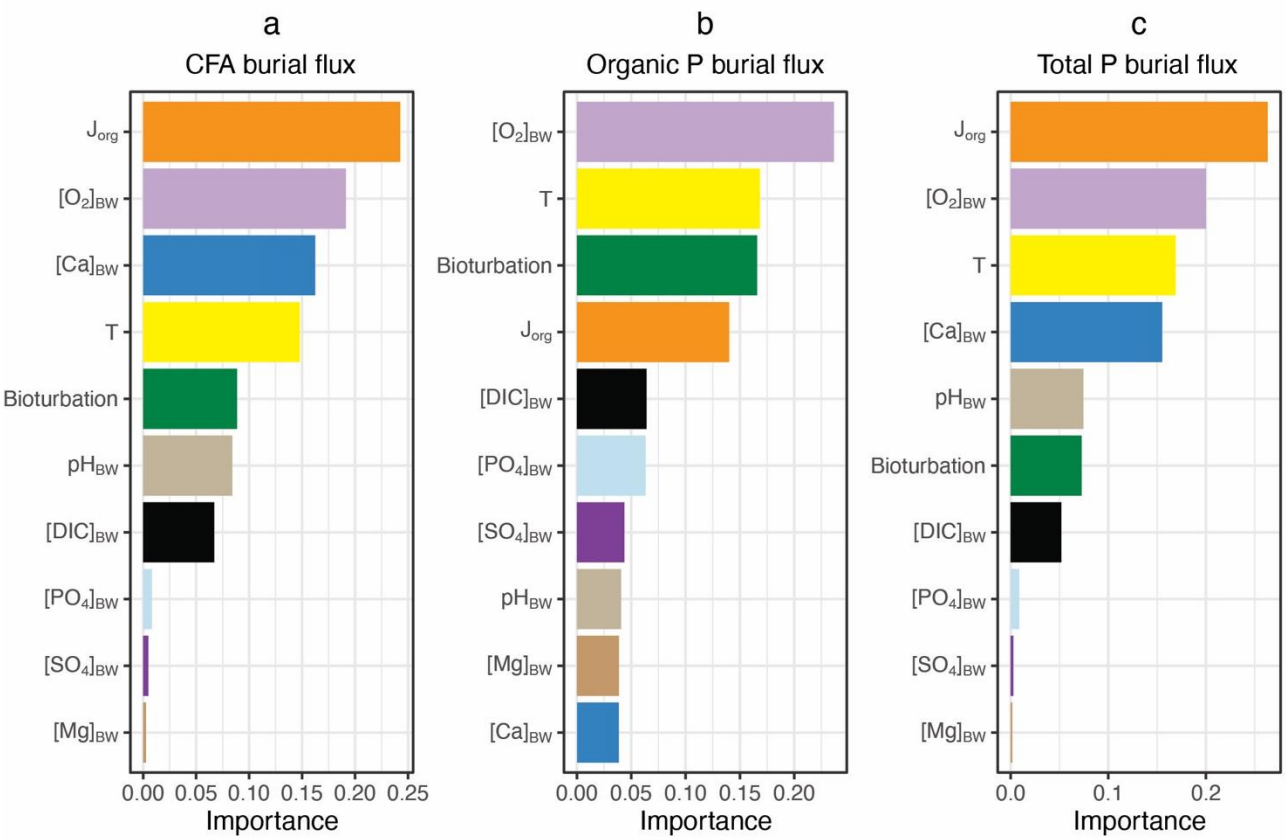

References:

1 Elser, J. J. *et al.* Global analysis of nitrogen and phosphorus limitation of primary producers in freshwater, marine and terrestrial ecosystems. *Ecol. Lett.* **10**, 1135-1142 (2007).

2 Vitousek, P. M., Porder, S., Houlton, B. Z. & Chadwick, O. A. Terrestrial phosphorus limitation: mechanisms, implications, and nitrogen-phosphorus interactions. *Ecol. Appl.* **20**, 5-15 (2010).
3 Du, E. Z. *et al.* Global patterns of terrestrial nitrogen and phosphorus limitation. *Nat. Geosci.* **13**, 221-228 (2020).
4 Tyrrell, T. The relative influences of nitrogen and phosphorus on oceanic primary production. *Nature* **400**, 525-531 (1999).
5 Ruttenberg, K. The global phosphorus cycle. *Treatise Geochem.* **8**, 682 (2003).
6 Meyer, K. M., Kump, L. R. & Ridgwell, A. Biogeochemical controls on photic-zone euxinia during the end-Permian mass extinction. *Geology* **36**, 747-750 (2008).
7 Lenton, T. M., Daine, S. J. & Mills, B. J. W. COPSE reloaded: An improved model of biogeochemical cycling over Phanerozoic time. *Earth Sci. Rev.* **178**, 1-28 (2018).
8 Komar, N. & Zeebe, R. E. Redox-controlled carbon and phosphorus burial: A mechanism for enhanced organic carbon sequestration during the PETM. *Earth Planet. Sci. Lett.* **479**, 71-82 (2017).
9 Föllmi, K. B. The phosphorus cycle, phosphogenesis and marine phosphate-rich deposits. *Earth Sci. Rev.* **40**, 55-124 (1996).
10 Paytan, A. & McLaughlin, K. The oceanic phosphorus cycle. *Chem. Rev.* **107**, 563-576 (2007).
11 Filippelli, G. M. The global phosphorus cycle: Past, present, and future. *Elements* **4**, 89-95 (2008).
12 Zhao, M. Y., Zhang, S., Tarhan, L. G., Reinhard, C. T. & Planavsky, N. The role of calcium in regulating marine phosphorus burial and atmospheric oxygenation. *Nat. Commun.* **11**, 2232 (2020).
13 Papadomanolaki, N. M., Lenstra, W. K., Wolthers, M. & Slomp, C. P. Enhanced phosphorus recycling during past oceanic anoxia amplified by low rates of apatite authigenesis. *Sci. Adv.* **8**, eabn2370 (2022).
14 Sharoni, S. & Halevy, I. Geologic controls on phytoplankton elemental composition. *Proc. Nat. Acad. Sci. U.S.A.* **119**, e2113263118 (2022).
15 Walton, C. R. *et al.* Evolution of the crustal phosphorus reservoir. *Sci. Adv.* **9**, eade6923 (2023).
16 Dodd, M. S. *et al.* Uncovering the Ediacaran phosphorus cycle. *Nature* **618**, 974-980 (2023).
17 Walker, T. & Syers, J. K. The fate of phosphorus during pedogenesis. *Geoderma* **15**, 1-19 (1976).
18 Föllmi, K. B., Hosein, R., Arn, K. & Steinmann, P. Weathering and the mobility of phosphorus in the catchments and forefields of the Rhône and Oberaar glaciers, central Switzerland: implications for the global phosphorus cycle on glacial–interglacial timescales. *Geochim. Cosmochim. Acta* **73**, 2252-2282 (2009).
19 He, X. J. *et al.* Global patterns and drivers of soil total phosphorus concentration. *Earth Syst. Sci. Data* **13**, 5831-5846 (2021).
20 Guidry, M. W. & Mackenzie, F. T. Apatite weathering and the Phanerozoic phosphorus cycle. *Geology* **28**, 631-634 (2000).
21 Bergman, N. M., Lenton, T. M. & Watson, A. J. COPSE: A new model of biogeochemical cycling over Phanerozoic time. *Am. J. Sci.* **304**, 397-437 (2004).
22 Zhao, M. Y., Mills, B. J. W., Homoky, W. B. & Peacock, C. L. Oxygenation of the Earth aided by mineral-organic carbon preservation. *Nat. Geosci.* **16**, 262-269 (2023).

23 Guo, L. *et al.* Acceleration of phosphorus weathering under warm climates. *Sci. Adv.* **10**, eadm7773 (2024).
24 Walton, C. R. *et al.* Phosphorus availability on the early Earth and the impacts of life. *Nat. Geosci.* **16**, 399-409 (2023).
25 Benitez-Nelson, C. R. The biogeochemical cycling of phosphorus in marine systems. *Earth Sci. Rev.* **51**, 109-135 (2000).
26 Ruttenberg, K. C. Reassessment of the oceanic residence time of phosphorus. *Chem. Geol.* **107**, 405-409 (1993).
27 Walton, C. R. *et al.* Phosphorus mineral evolution and prebiotic chemistry: From minerals to microbes. *Earth Sci. Rev.* **221**, 103806 (2021).
28 Hartmann, J., Moosdorf, N., Lauerwald, R., Hinderer, M. & West, A. J. Global chemical weathering and associated P-release—The role of lithology, temperature and soil properties. *Chem. Geol.* **363**, 145-163 (2014).
29 Beck, M. A. & Sanchez, P. A. Soil phosphorus fraction dynamics during 18 years of cultivation on a Typic Paleudult. *Soil Sci. Soc. Am. J.* **58**, 1424-1431 (1994).
30 Bortoluzzi, E. C., Pérez, C. A. S., Ardisson, J. D., Tiecher, T. & Caner, L. Occurrence of iron and aluminum sesquioxides and their implications for the P sorption in subtropical soils. *Appl. Clay Sci.* **104**, 196-204 (2015).
31 Fink, J. R., Inda, A. V., Tiecher, T. & Barrón, V. Iron oxides and organic matter on soil phosphorus availability. *Cienc. Agrotecnologia* **40**, 369-379 (2016).
32 Wardle, D. A., Walker, L. R. & Bardgett, R. D. Ecosystem properties and forest decline in contrasting long-term chronosequences. *Science* **305**, 509-513 (2004).
33 Lenton, T. M., Crouch, M., Johnson, M., Pires, N. & Dolan, L. First plants cooled the Ordovician. *Nat. Geosci.* **5**, 86-89 (2012).
34 Berner, R. A. & Rao, J.-L. Phosphorus in sediments of the Amazon River and estuary: Implications for the global flux of phosphorus to the sea. *Geochim. Cosmochim. Acta* **58**, 2333-2339 (1994).
35 Lebo, M. E. Particle-bound phosphorus along an urbanized coastal plain estuary. *Mar. Chem.* **34**, 225-246 (1991).
36 Feely, R. A., Trefry, J. H., Lebon, G. T. & German, C. R. The relationship between P/Fe and V/Fe ratios in hydrothermal precipitates and dissolved phosphate in seawater. *Geophys. Res. Lett.* **25**, 2253-2256 (1998).
37 Hao, W. *et al.* The kaolinite shuttle links the Great Oxidation and Lomagundi events. *Nat. Commun.* **12**, 2944 (2021).
38 Fru, E. C. *et al.* Transient fertilization of a post-Sturtian Snowball ocean margin with dissolved phosphate by clay minerals. *Nat. Commun.* **14**, 8418 (2023).
39 Lal, D. & Lee, T. Cosmogenic ^{32}P and ^{33}P used as tracers to study phosphorus recycling in the upper ocean. *Nature* **333**, 752-754 (1988).
40 Dyhrman, S. T. *et al.* Phosphonate utilization by the globally important marine diazotroph. *Nature* **439**, 68-71 (2006).
41 Diaz, J. *et al.* Marine polyphosphate: A key player in geologic phosphorus sequestration. *Science* **320**, 652-655 (2008).
42 Inomura, K., Deutsch, C., Jahn, O., Dutkiewicz, S. & Follows, M. J. Global patterns in marine organic matter stoichiometry driven by phytoplankton ecophysiology. *Nat. Geosci.* **15**, 1034-1040 (2022).
43 Martiny, A. C. *et al.* Biogeochemical controls of surface ocean phosphate. *Sci. Adv.* **5**, eaax0341 (2019).

44 Ruttenberg, K. C. & Berner, R. A. Authigenic apatite formation and burial in sediments from non-upwelling, continental margin environments. *Geochim. Cosmochim. Acta* **57**, 991-1007 (1993).

45 Slomp, C. P., Epping, E. H. G., Helder, W. & VanRaaphorst, W. A key role for iron-bound phosphorus in authigenic apatite formation in North Atlantic continental platform sediments. *J. Mar. Res.* **54**, 1179-1205 (1996).

46 Reed, D. C., Slomp, C. P. & Gustafsson, B. G. Sedimentary phosphorus dynamics and the evolution of bottom-water hypoxia: A coupled benthic-pelagic model of a coastal system. *Limnol. Oceanogr.* **56**, 1075-1092 (2011).

47 Dale, A. W., Boyle, R. A., Lenton, T. M., Ingall, E. D. & Wallmann, K. A model for microbial phosphorus cycling in bioturbated marine sediments: Significance for phosphorus burial in the early Paleozoic. *Geochim. Cosmochim. Acta* **189**, 251-268 (2016).

48 Berner, R. A. Phosphate removal from sea water by adsorption on volcanogenic ferric oxides. *Earth Planet. Sci. Lett.* **18**, 77-86 (1973).

49 Feely, R. A. *et al.* The effect of hydrothermal processes on midwater phosphorus distributions in the northeast Pacific. *Earth Planet. Sci. Lett.* **96**, 305-318 (1990).

50 Poulton, S. W. & Canfield, D. E. Co-diagenesis of iron and phosphorus in hydrothermal sediments from the southern East Pacific Rise: Implications for the evaluation of paleoseawater phosphate concentrations. *Geochim. Cosmochim. Acta* **70**, 5883-5898 (2006).

51 März, C., Poulton, S. W., Wagner, T., Schnetger, B. & Brumsack, H.-J. Phosphorus burial and diagenesis in the central Bering Sea (Bowers Ridge, IODP Site U1341): perspectives on the marine P cycle. *Chem. Geol.* **363**, 270-282 (2014).

52 Latimer, J. C., Filippelli, G. M., Hendy, I. & Newkirk, D. R. Opal-associated particulate phosphorus: Implications for the marine P cycle. *Geochim. Cosmochim. Acta* **70**, 3843-3854 (2006).

53 Eijsink, L., Krom, M. & De Lange, G. The use of sequential extraction techniques for sedimentary phosphorus in eastern Mediterranean sediments. *Mar. Geol.* **139**, 147-155 (1997).

54 Zhao, M.-Y., Zheng, Y.-F. & Zhao, Y.-Y. Seeking a geochemical identifier for authigenic carbonate. *Nat. Commun.* **7**, 10885 (2016).

55 Filippelli, G. M. & Delaney, M. L. Phosphorus geochemistry of equatorial Pacific sediments. *Geochim. Cosmochim. Acta* **60**, 1479-1495 (1996).

56 Delaney, M. L. Phosphorus accumulation in marine sediments and the oceanic phosphorus cycle. *Global Biogeochem. Cycles* **12**, 563-572 (1998).

57 Filippelli, G. M. Phosphate rock formation and marine phosphorus geochemistry: The deep time perspective. *Chemosphere* **84**, 759-766 (2011).

58 Compton, J. *et al.* Variations in the global phosphoruscycle. *SEPM Spec. Publ.* **66**, 21-33 (2000).

59 Berner, R. A. The rise of plants and their effect on weathering and atmospheric CO_2. *Science* **276**, 544-546 (1997).

60 Van Cappellen, P. & Ingall, E. D. Redox stabilization of the atmosphere and oceans by phosphorus-limited marine productivity. *Science* **271**, 493-496 (1996).

61 Guidry, M. W. & Mackenzie, F. T. Experimental study of igneous and sedimentary apatite dissolution: Control of pH, distance from equilibrium, and temperature on dissolution rates. *Geochim. Cosmochim. Acta* **67**, 2949-2963 (2003).

62 Chaïrat, C., Schott, J., Oelkers, E. H., Lartigue, J. E. & Harouiya, N. Kinetics and mechanism of natural fluorapatite dissolution at 25 °C and pH from 3 to 12. *Geochim. Cosmochim. Acta* **71**, 5901-5912 (2007).
63 Cox, G. M., Lyons, T. W., Mitchell, R. N., Hasterok, D. & Gard, M. Linking the rise of atmospheric oxygen to growth in the continental phosphorus inventory. *Earth Planet. Sci. Lett.* **489**, 28-36 (2018).
64 Algeo, T. J. & Twitchett, R. J. Anomalous Early Triassic sediment fluxes due to elevated weathering rates and their biological consequences. *Geology* **38**, 1023-1026 (2010).
65 Dal Corso, J. *et al.* Permo–Triassic boundary carbon and mercury cycling linked to terrestrial ecosystem collapse. *Nat. Commun.* **11**, 2962 (2020).
66 Tamburini, F. & Föllmi, K. B. Phosphorus burial in the ocean over glacial-interglacial time scales. *Biogeosciences* **6**, 501-513 (2009).
67 Chang, S. B. & Berner, R. A. Coal weathering and the geochemical carbon cycle. *Geochim. Cosmochim. Acta* **63**, 3301-3310 (1999).
68 Bolton, E. W., Berner, R. A. & Petsch, S. T. The weathering of sedimentary organic matter as a control on atmospheric O_2 II.: Theoretical modeling. *Am. J. Sci.* **306**, 575-615 (2006).
69 Zondervan, J. R. *et al.* Rock organic carbon oxidation CO_2 release offsets silicate weathering sink. *Nature* **623**, 329-333 (2023).
70 Yang, X., Post, W. M., Thornton, P. E. & Jain, A. The distribution of soil phosphorus for global biogeochemical modeling. *Biogeosciences* **10**, 2525-2537 (2013).
71 Augusto, L., Achat, D. L., Jonard, M., Vidal, D. & Ringeval, B. Soil parent material-A major driver of plant nutrient limitations in terrestrial ecosystems. *Glob. Change Biol.* **23**, 3808-3824 (2017).
72 Delgado-Baquerizo, M. *et al.* The influence of soil age on ecosystem structure and function across biomes. *Nat. Commun.* **11**, 4721 (2020).
73 Condie, K. C., Arndt, N., Davaille, A. & Puetz, S. J. Zircon age peaks: Production or preservation of continental crust? *Geosphere* **13**, 227-234 (2017).
74 Collerson, K. D. & Kamber, B. S. Evolution of the continents and the atmosphere inferred from Th-U-Nb systematics of the depleted mantle. *Science* **283**, 1519-1522 (1999).
75 Korenaga, J., Planavsky, N. J. & Evans, D. A. D. Global water cycle and the coevolution of the Earth's interior and surface environment. *Phil. Trans. R. Soc. A.* **375**, 20150393 (2017).
76 McLennan, S. M. & Taylor, S. Geochemical constraints on the growth of the continental crust. *The Journal of Geology* **90**, 347-361 (1982).
77 Tang, M., Chu, X., Hao, J. H. & Shen, B. Orogenic quiescence in Earth's middle age. *Science* **371**, 728-731 (2021).
78 Scotese, C. R., Song, H. J., Mills, B. J. W. & van der Meer, D. G. Phanerozoic paleotemperatures: The earth's changing climate during the last 540 million years. *Earth Sci. Rev.* **215** (2021).
79 Hoffman, P. F. *et al.* Snowball Earth climate dynamics and Cryogenian geology-geobiology. *Sci. Adv.* **3** (2017).
80 Yuan, W. *et al.* Mercury isotopes show vascular plants had colonized land extensively by the early Silurian. *Sci. Adv.* **9**, eade9510 (2023).
81 Syverson, D. D. *et al.* Nutrient supply to planetary biospheres from anoxic weathering of mafic oceanic crust. *Geophys. Res. Lett.* **48**, e2021GL094442 (2021).

82 Berner, R. A. & Caldeira, K. The need for mass balance and feedback in the geochemical carbon cycle. *Geology* **25**, 955-956 (1997).
83 D'Antonio, M. P., Ibarra, D. E. & Boyce, C. K. Land plant evolution decreased, rather than increased, weathering rates. *Geology* **48**, 29-33 (2020).
84 Sharoni, S. & Halevy, I. Rates of seafloor and continental weathering govern Phanerozoic marine phosphate levels. *Nat. Geosci.* **16**, 75-81 (2023).
85 Ma, C., Tang, Y. & Ying, J. Global tectonics and oxygenation events drove the Earth-scale phosphorus cycle. *Earth Sci. Rev.* **233**, 104166 (2022).
86 Cheng, Y. T. *et al.* Spatial distribution of soil total phosphorus in Yingwugou watershed of the Dan River, China. *Catena* **136**, 175-181 (2016).
87 Guilbaud, R. *et al.* Phosphorus-limited conditions in the early Neoproterozoic ocean maintained low levels of atmospheric oxygen. *Nat. Geosci.* **13**, 296-301 (2020).
88 Bucholz, C. E. Coevolution of sedimentary and strongly peraluminous granite phosphorus records. *Earth Planet. Sci. Lett.* **596**, 117795 (2022).
89 Wan, B. *et al.* Seismological evidence for the earliest global subduction network at 2 Ga ago. *Sci. Adv.* **6**, eabc5491 (2020).
90 Horton, F. Did phosphorus derived from the weathering of large igneous provinces fertilize the Neoproterozoic ocean? *Geochem. Geophys. Geosyst.* **16**, 1723-1738 (2015).
91 Porder, S. & Ramachandran, S. The phosphorus concentration of common rocks—a potential driver of ecosystem P status. *Plant Soil* **367**, 41-55 (2013).
92 Sun, H. *et al.* Rapid enhancement of chemical weathering recorded by extremely light seawater lithium isotopes at the Permian-Triassic boundary. *Proc. Nat. Acad. Sci. U.S.A.* **115**, 3782-3787 (2018).
93 Longman, J., Mills, B. J. W., Manners, H. R., Gernon, T. M. & Palmer, M. R. Late Ordovician climate change and extinctions driven by elevated volcanic nutrient supply. *Nat. Geosci.* **14**, 924-929 (2021).
94 Ma, C., Tang, Y. J. & Ying, J. F. Volcanic phosphorus spikes associated with supercontinent assembly supported the evolution of land plants. *Earth Sci. Rev.* **232**, 104101 (2022).
95 Achat, D. L., Pousse, N., Nicolas, M., Brédoire, F. & Augusto, L. Soil properties controlling inorganic phosphorus availability: general results from a national forest network and a global compilation of the literature. *Biogeochemistry* **127**, 255-272 (2016).
96 Mehmood, A., Akhtar, M. S., Imran, M. & Rukh, S. Soil apatite loss rate across different parent materials. *Geoderma* **310**, 218-229 (2018).
97 Siqueira, R. G. *et al.* Weathering and pedogenesis of sediments and basaltic rocks on Vega Island, Antarctic Peninsula. *Geoderma* **382**, 114707 (2021).
98 Stallard, R. F. Tectonic, environmental, and human aspects of weathering and erosion: a global review using a steady-state perspective. *Annu. Rev. Earth Planet. Sci.* **23**, 11-39 (1995).
99 Goddéris, Y. *et al.* Onset and ending of the late Palaeozoic ice age triggered by tectonically paced rock weathering. *Nature Geoscience* **10**, 382-386 (2017).
100 Porder, S. & Chadwick, O. A. Climate and soil-age constraints on nutrient uplift and retention by plants. *Ecology* **90**, 623-636 (2009).
101 Harouiya, N., Chaïrat, C., Köhler, S. J., Gout, R. & Oelkers, E. H. The dissolution kinetics and apparent solubility of natural apatite in closed reactors at temperatures from 5 to 50 °C and pH from 1 to 6. *Chem. Geol.* **244**, 554-568 (2007).

102 West, A. J. Thickness of the chemical weathering zone and implications for erosional and climatic drivers of weathering and for carbon-cycle feedbacks. *Geology* **40**, 811-814 (2012).
103 Maffre, P. *et al.* Mountain ranges, climate and weathering. Do orogens strengthen or weaken the silicate weathering carbon sink? *Earth Planet. Sci. Lett.* **493**, 174-185 (2018).
104 Hou, E. *et al.* Effects of climate on soil phosphorus cycle and availability in natural terrestrial ecosystems. *Glob. Change Biol* **24**, 3344-3356 (2018).
105 Sims, J., Simard, R. & Joern, B. Phosphorus loss in agricultural drainage: Historical perspective and current research. *J. Environ. Qual.* **27**, 277-293 (1998).
106 Mills, B. J. W., Donnadieu, Y. & Goddéris, Y. Spatial continuous integration of Phanerozoic global biogeochemistry and climate. *Gondwana Res.* **100**, 73-86 (2021).
107 Goddéris, Y., Donnadieu, Y. & Mills, B. J. W. What models tell us about the evolution of carbon sources and sinks over the Phanerozoic. *Annu. Rev. Earth Planet. Sci.* **51**, 471-492 (2023).
108 Ozaki, K. & Tajika, E. Biogeochemical effects of atmospheric oxygen concentration, phosphorus weathering, and sea-level stand on oceanic redox chemistry: Implications for greenhouse climates. *Earth Planet. Sci. Lett.* **373**, 129-139 (2013).
109 Hülse, D. *et al.* End-Permian marine extinction due to temperature-driven nutrient recycling and euxinia. *Nat. Geosci.* **14**, 862-867 (2021).
110 Wu, X. J. *et al.* Genome-resolved metagenomics reveals distinct phosphorus acquisition strategies between soil microbiomes. *Msystems* **7**, e0110721 (2022).
111 Yao, Q. M. *et al.* Community proteogenomics reveals the systemic impact of phosphorus availability on microbial functions in tropical soil. *Nat. Ecol. Evol.* **2**, 499-509 (2018).
112 Planavsky, N. J. *et al.* Evolution of the structure and impact of Earth's biosphere. *Nat. Rev. Earth Environ.* **2**, 123-139 (2021).
113 Retallack, G. J. Early forest soils and their role in Devonian global change. *Science* **276**, 583-585 (1997).
114 Moulton, K. L. & Berner, R. A. Quantification of the effect of plants on weathering: Studies in Iceland. *Geology* **26**, 895-898 (1998).
115 Algeo, T. J. & Scheckler, S. E. Terrestrial-marine teleconnections in the Devonian: links between the evolution of land plants, weathering processes, and marine anoxic events. *Philos. Trans. R. Soc. B Biol. Sci.* **353**, 113-128 (1998).
116 Filippelli, G. M. The global phosphorus cycle. *Rev. Mineral. Geochem.* **48**, 391-425 (2002).
117 Quirk, J. *et al.* Constraining the role of early land plants in Palaeozoic weathering and global cooling. *Proc. R. Soc. B Biol. Sci.* **282**, 20151115 (2015).
118 Berner, R. A. Weathering, plants, and the long-term carbon cycle. *Geochim. Cosmochim. Acta* **56**, 3225-3231 (1992).
119 Slessarev, E. W. *et al.* Water balance creates a threshold in soil pH at the global scale. *Nature* **540**, 567-569 (2016).
120 Seitzinger, S. P., Harrison, J. A., Dumont, E., Beusen, A. H. W. & Bouwman, A. F. Sources and delivery of carbon, nitrogen, and phosphorus to the coastal zone: An overview of Global Nutrient Export from Watersheds (NEWS) models and their application. *Global Biogeochem. Cycles* **19**, GB4S01 (2005).

121 Kolowith, L. C. & Berner, R. A. Weathering of phosphorus in black shales. *Global Biogeochem. Cycles* **16**, 1140 (2002).
122 Laakso, T. A. & Schrag, D. P. Regulation of atmospheric oxygen during the Proterozoic. *Earth Planet. Sci. Lett.* **388**, 81-91 (2014).
123 Colman, A. S. & Holland, H. D. in *Marine Authigenesis: From Global to Microbial* (ed Liliane Prévôt-Lucas Craig R. Glenn, Jacques Lucas) (SEPM SPECIAL PUBLICATION, 2000).
124 Ingall, E. & Jahnke, R. Evidence for enhanced phosphorus regeneration from marine sediments overlain by oxygen depleted waters. *Geochim. Cosmochim. Acta* **58**, 2571-2575 (1994).
125 Tsandev, I., Reed, D. C. & Slomp, C. P. Phosphorus diagenesis in deep-sea sediments: Sensitivity to water column conditions and global scale implications. *Chem. Geol.* **330**, 127-139 (2012).
126 Schenau, S., Reichart, G.-J. & De Lange, G. Phosphorus burial as a function of paleoproductivity and redox conditions in Arabian Sea sediments. *Geochim. Cosmochim. Acta* **69**, 919-931 (2005).
127 Zhao, M. Y., Tarhan, L., Planavsky, N. & Isson, T. The influence of warming on phosphorus burial in continental margin sediments. *Am. J. Sci.* **323**, 6 (2023).
128 Van Cappellen, P. & Berner, R. A. Fluorapatite crystal growth from modified seawater solutions. *Geochim. Cosmochim. Acta* **55**, 1219-1234 (1991).
129 Boyle, R. A. *et al.* Stabilization of the coupled oxygen and phosphorus cycles by the evolution of bioturbation. *Nat. Geosci.* **7**, 671-676 (2014).
130 Tarhan, L. G., Zhao, M. & Planavsky, N. J. Bioturbation feedbacks on the phosphorus cycle. *Earth Planet. Sci. Lett.* **566**, 116961 (2021).
131 Bjerrum, C. J. & Canfield, D. E. Ocean productivity before about 1.9 Gyr ago limited by phosphorus adsorption onto iron oxides. *Nature* **417**, 159-162 (2002).
132 Jones, C., Nomosatryo, S., Crowe, S. A., Bjerrum, C. J. & Canfield, D. E. Iron oxides, divalent cations, silica, and the early earth phosphorus crisis. *Geology* **43**, 135-138 (2015).
133 Derry, L. A. Causes and consequences of mid-Proterozoic anoxia. *Geophys. Res. Lett.* **42**, 8538-8546 (2015).
134 Xiong, Y. J., Guilbaud, R., Peacock, C. L., Krom, M. D. & Poulton, S. W. Phosphorus controls on the formation of vivianite versus green rust under anoxic conditions. *Geochim. Cosmochim. Acta* **351**, 139-151 (2023).
135 Reinhard, C. T. *et al.* Evolution of the global phosphorus cycle. *Nature* **541**, 386-389 (2017).
136 Nathan, Y., Bremner, J. M., Lowenthal, R. E. & Monteiro, P. Role of Bacteria in Phosphorite Genesis. *Geomicrobiol. J.* **11**, 69-76 (1993).
137 Schulz, H. N. & Schulz, H. D. Large sulfur bacteria and the formation of phosphorite. *Science* **307**, 416-418 (2005).
138 Goldhammer, T., Brüchert, V., Ferdelman, T. G. & Zabel, M. Microbial sequestration of phosphorus in anoxic upwelling sediments. *Nat. Geosci.* **3**, 557-561 (2010).
139 Lepland, A. *et al.* Potential influence of sulphur bacteria on Palaeoproterozoic phosphogenesis. *Nat. Geosci.* **7**, 20-24 (2014).
140 Herschy, B. *et al.* Archean phosphorus liberation induced by iron redox geochemistry. *Nat. Commun.* **9**, 1346 (2018).
141 Planavsky, N. J. *et al.* A sedimentary record of the evolution of the global marine phosphorus cycle. *Geobiology* **21**, 168-174 (2023).

142 Laakso, T. A., Sperling, E. A., Johnston, D. T. & Knoll, A. H. Ediacaran reorganization of the marine phosphorus cycle. *Proc. Nat. Acad. Sci. U.S.A.* **117**, 11961-11967 (2020).
143 McClellan, G. & Van Kauwenbergh, S. Mineralogical and chemical variation of francolites with geological time. *J. Geol. Soc.* **148**, 809-812 (1991).
144 Lenton, T. M., Boyle, R. A., Poulton, S. W., Shields-Zhou, G. A. & Butterfield, N. J. Co-evolution of eukaryotes and ocean oxygenation in the Neoproterozoic era. *Nat. Geosci.* **7**, 257-265 (2014).
145 Henrichs, S. M. & Reeburgh, W. S. Anaerobic mineralization of marine sediment organic matter: rates and the role of anaerobic processes in the oceanic carbon economy. *Geomicrobiol. J.* **5**, 191-237 (1987).
146 Betts, J. N. & Holland, H. D. The oxygen content of ocean bottom waters, the burial efficiency of organic carbon, and the regulation of atmospheric oxygen. *Glob. Planet. Change.* **97**, 5-18 (1991).
147 Canfield, D. E. Sulfate reduction and oxic respiration in marine sediments: implications for organic carbon preservation in euxinic environments. *Deep-Sea Res. Part A Oceanogr. Res. Pap.* **36**, 121-138 (1989).
148 Schoepfer, S. D. *et al.* Total organic carbon, organic phosphorus, and biogenic barium fluxes as proxies for paleomarine productivity. *Earth Sci. Rev.* **149**, 23-52 (2015).
149 Aller, R. C. Diagenetic processes near the sediment-water interface of Long Island sound. I.: Decomposition and nutrient element geochemistry (S, N, P). *Adv. Geophys.* **22**, 237-350 (1980).
150 Westrich, J. T. & Berner, R. A. The effect of temperature on rates of sulfate reduction in marine sediments. *Geomicrobiol. J.* **6**, 99-117 (1988).
151 Middelburg, J. J. *et al.* Organic matter mineralization in intertidal sediments along an estuarine gradient. *Mar. Ecol. Prog. Ser.* **132**, 157-168 (1996).
152 Burdige, D. J. Temperature dependence of organic matter remineralization in deeply-buried marine sediments. *Earth Planet. Sci. Lett.* **311**, 396-410 (2011).
153 Burnett, W. C. Apatite-glauconite associations off Peru and Chile: palaeo-oceanograpic implications. *J. Geol. Soc.* **137**, 757-764 (1980).
154 Garrison, R. E. & Kastner, M. Phosphatic sediments and rocks recovered from the Peru margin during ODP Leg 112. *Proc. Ocean Drill. Program Sci. Results* **112**, 111-134 (1990).
155 Shimmield, G. & Mowbray, S. The inorganic geochemical record of the northwest Arabian Sea: A history of productivity variation over the last 400 ky from site 722 and 724. *Proc. Ocean Drill. Program Sci. Results* **117**, 409-429 (1991).
156 Schenau, S., Slomp, C. P. & DeLange, G. J. Phosphogenesis and active phosphorite formation in sediments from the Arabian Sea oxygen minimum zone. *Mar. Geol.* **169**, 1-20 (2000).
157 Ganeshram, R. S., Pedersen, T. F., Calvert, S. E. & Francois, R. Reduced nitrogen fixation in the glacial ocean inferred from changes in marine nitrogen and phosphorus inventories. *Nature* **415**, 156-159 (2002).
158 Jahnke, R. A. The synthesis and solubility of carbonate fluorapatite. *Am. J. Sci.* **284**, 58-78 (1984).
159 Dickson, J. A. D. Fossil echinoderms as monitor of the Mg/Ca ratio of phanerozoic oceans. *Science* **298**, 1222-1224 (2002).

160 Horita, J., Zimmermann, H. & Holland, H. D. Chemical evolution of seawater during the Phanerozoic: Implications from the record of marine evaporites. *Geochim. Cosmochim. Acta* **66**, 3733-3756 (2002).
161 Coggon, R. M., Teagle, D. A. H., Smith-Duque, C. E., Alt, J. C. & Cooper, M. J. Reconstructing past seawater Mg/Ca and Sr/Ca from mid-ocean ridge flank calcium carbonate veins. *Science* **327**, 1114-1117 (2010).
162 Nelson, B. W. Sedimentary phosphate method for estimating paleosalinities. *Science* **158**, 917-920 (1967).
163 Weng, H. X., Presley, B. J. & Armstrong, D. Distribution of sedimentary phosphorus in Gulf of Mexico estuaries. *Mar. Environ. Res.* **37**, 375-392 (1994).
164 Faul, K. L., Paytan, A. & Wilson, P. Phosphorus and barite concentrations and geochemistry in Site 1221 Paleocene/Eocene boundary sediments. *Proc. Ocean Drill. Program Sci. Results* **199**, 1-23 (2005).
165 Heggie, D. *et al.* Organic carbon cycling and modern phosphorite formation on the East Australian continental margin: an overview. *Geol. Soc. Spec. Publ.* **52**, 87-117 (1990).
166 Schuffert, J. D. *et al.* Rates of formation of modern phosphorite off western Mexico. *Geochim. Cosmochim. Acta* **58**, 5001-5010 (1994).
167 Isson, T. T. & Planavsky, N. J. Reverse weathering as a long-term stabilizer of marine pH and planetary climate. *Nature* **560**, 471-475 (2018).
168 Van Cappellen, P. & Ingall, E. D. Benthic phosphorus regeneration, net primary production, and ocean anoxia: a model of the coupled marine biogeochemical cycles of carbon and phosphorus. *Paleoceanography* **9**, 677-692 (1994).
169 Mort, H. P. *et al.* Phosphorus and the roles of productivity and nutrient recycling during oceanic anoxic event 2. *Geology* **35**, 483-486 (2007).
170 Poulton, S. W. *et al.* A continental-weathering control on orbitally driven redox-nutrient cycling during Cretaceous Oceanic Anoxic Event 2. *Geology* **43**, 963-966 (2015).
171 Algeo, T. J. & Ingall, E. Sedimentary C_{org}:P ratios, paleocean ventilation, and Phanerozoic atmospheric pO_2. *Palaeogeog. Palaeoclimatol. Palaeoecol.* **256**, 130-155 (2007).
172 Monbet, P., Brunskill, G., Zagorskis, I. & Pfitzner, J. Phosphorus speciation in the sediment and mass balance for the central region of the Great Barrier Reef continental shelf (Australia). *Geochim. Cosmochim. Acta* **71**, 2762-2779 (2007).
173 Slomp, C. P. & Van Cappellen, P. The global marine phosphorus cycle: sensitivity to oceanic circulation. *Biogeosciences* **4**, 155-171 (2007).
174 Alcott, L. J., Mills, B. J. W. & Poulton, S. W. Stepwise Earth oxygenation is an inherent property of global biogeochemical cycling. *Science* **366**, 1333-1337 (2019).
175 Jiang, L. *et al.* Pulses of atmosphere oxygenation during the Cambrian radiation of animals. *Earth Planet. Sci. Lett.* **590**, 117565 (2022).
176 Poulton, S. W. Early phosphorus redigested. *Nat. Geosci.* **10**, 75-76 (2017).
177 Schobben, M. *et al.* A nutrient control on marine anoxia during the end-Permian mass extinction. *Nat. Geosci.* **13**, 640-646 (2020).
178 Qiu, Z. *et al.* A nutrient control on expanded anoxia and global cooling during the Late Ordovician mass extinction. *Commun. Earth Environ.* **3**, 82 (2022).
179 Cauwet, G. Organic-chemistry of sea-water particulates concepts and developments. *Oceanol. Acta* **1**, 99-105 (1978).

180 Poulton, S. W. & Canfield, D. E. Ferruginous conditions: a dominant feature of the ocean through Earth's history. *Elements* **7**, 107-112 (2011).
181 Sperling, E. A. *et al.* Statistical analysis of iron geochemical data suggests limited late Proterozoic oxygenation. *Nature* **523**, 451-454 (2015).
182 Zegeye, A. *et al.* Green rust formation controls nutrient availability in a ferruginous water column. *Geology* **40**, 599-602 (2012).
183 Konhauser, K. O., Lalonde, S. V., Amskold, L. & Holland, H. D. Was there really an Archean phosphate crisis? *Science* **315**, 1234-1234 (2007).
184 Alcott, L. J., Mills, B. J., Bekker, A. & Poulton, S. W. Earth's Great Oxidation Event facilitated by the rise of sedimentary phosphorus recycling. *Nat. Geosci.* **15**, 210-215 (2022).
185 Song, Y. *et al.* Dynamic redox and nutrient cycling response to climate forcing in the Mesoproterozoic ocean. *Nat. Commun.* **14**, 6640 (2023).
186 Cosmidis, J. *et al.* Biomineralization of iron-phosphates in the water column of Lake Pavin (Massif Central, France). *Geochim. Cosmochim. Acta* **126**, 78-96 (2014).
187 Vuillemin, A. *et al.* Vivianite formation in ferruginous sediments from Lake Towuti, Indonesia. *Biogeosciences* **17**, 1955-1973 (2020).
188 Johnson, B. R. *et al.* Phosphorus burial in ferruginous SiO_2-rich Mesoproterozoic sediments. *Geology* **48**, 92-96 (2020).
189 van de Velde, S., Mills, B. J. W., Meysman, F. J. R., Lenton, T. M. & Poulton, S. W. Early Palaeozoic ocean anoxia and global warming driven by the evolution of shallow burrowing. *Nat. Commun.* **9**, 2554 (2018).
190 Dahl, T. W. *et al.* Atmosphere-ocean oxygen and productivity dynamics during early animal radiations. *Proc. Nat. Acad. Sci. U.S.A.* **116**, 19352-19361 (2019).
191 Cribb, A. T., van de Velde, S. J., Berelson, W. M., Bottjer, D. J. & Corsetti, F. A. Ediacaran–Cambrian bioturbation did not extensively oxygenate sediments in shallow marine ecosystems. *Geobiology* **21**, 435-453 (2023).
192 Meysman, F. J., Boudreau, B. P. & Middelburg, J. J. Relations between local, nonlocal, discrete and continuous models of bioturbation. *J. Mar. Res.* **61**, 391-410 (2003).
193 Aller, R. C. Quantifying solute distributions in the bioturbated zone of marine sediments by defining an average microenvironment. *Geochim. Cosmochim. Acta* **44**, 1955-1965 (1980).
194 Boudreau, B. P. On the equivalence of nonlocal and radial-diffusion models for porewater irrigation. *J. Mar. Res.* **42**, 731-735 (1984).
195 Rivas-Lamelo, S. *et al.* Magnetotactic bacteria as a new model for P sequestration in the ferruginous Lake Pavin. *Geochem. Perspect. Lett.* **5**, 35-41 (2017).
196 Brock, J. & Schulz-Vogt, H. N. Sulfide induces phosphate release from polyphosphate in cultures of a marine Beggiatoa strain. *ISME J.* **5**, 497-506 (2011).
197 Butterfield, N. J. Oxygen, animals and oceanic ventilation: an alternative view. *Geobiology* **7**, 1-7 (2009).
198 Fakhraee, M., Planavsky, N. J. & Reinhard, C. T. The role of environmental factors in the long-term evolution of the marine biological pump. *Nat. Geosci.* **13**, 812-816 (2020).
199 Redfield, A. C. The biological control of chemical factors in the environment. *Am. Sci.* **46**, 205-221 (1958).
200 Arrigo, K. R. Marine microorganisms and global nutrient cycles. *Nature* **437**, 349-355 (2005).

201 Martiny, A. C. *et al.* Strong latitudinal patterns in the elemental ratios of marine plankton and organic matter. *Nat. Geosci.* **6**, 279-283 (2013).
202 Weber, T. S. & Deutsch, C. Ocean nutrient ratios governed by plankton biogeography. *Nature* **467**, 550-554 (2010).
203 Planavsky, N. J. The elements of marine life. *Nat. Geosci.* **7**, 855-856 (2014).
204 Galbraith, E. D. & Martiny, A. C. A simple nutrient-dependence mechanism for predicting the stoichiometry of marine ecosystems. *Proc. Nat. Acad. Sci. U.S.A.* **112**, 8199-8204 (2015).
205 Yvon-Durocher, G., Dossena, M., Trimmer, M., Woodward, G. & Allen, A. P. Temperature and the biogeography of algal stoichiometry. *Glob. Ecol. Biogeogr.* **24**, 562-570 (2015).
206 Cawley, J. L., Burruss, R. C. & Holland, H. D. Chemical weathering in central iceland: An analog of pre-silurian weathering. *Science* **165**, 391-392 (1969).
207 Volk, T. Feedbacks between weathering and atmospheric CO_2 over the last 100 million years. *Am. J. Sci.* **287**, 763-779 (1987).
208 Brantley, S. L., Shaughnessy, A., Lebedeva, M. I. & Balashov, V. N. How temperature-dependent silicate weathering acts as Earth's geological thermostat. *Science* **379**, 382-389 (2023).
209 Goddéris, Y., Donnadieu, Y., Le Hir, G., Lefebvre, V. & Nardin, E. The role of palaeogeography in the Phanerozoic history of atmospheric CO_2 and climate. *Earth Sci. Rev.* **128**, 122-138 (2014).
210 Kraal, P., Dijkstra, N., Behrends, T. & Slomp, C. P. Phosphorus burial in sediments of the sulfidic deep Black Sea: Key roles for adsorption by calcium carbonate and apatite authigenesis. *Geochim. Cosmochim. Acta* **204**, 140-158 (2017).
211 Kasting, J. F. Theoretical constraints on oxygen and carbon dioxide concentrations in the Precambrian atmosphere. *Precambrian Res.* **34**, 205-229 (1987).
212 Royer, D. L., Berner, R. A., Montañez, I. P., Tabor, N. J. & Beerling, D. J. CO_2 as a primary driver of phanerozoic climate. *GSA today* **14**, 4-10 (2004).
213 Rudnick, R. & Gao, S. Composition of the continental crust. *Treatise Geochem.* **3**, 1-64 (2013).
214 Lyons, T. W., Reinhard, C. T. & Planavsky, N. J. The rise of oxygen in Earth's early ocean and atmosphere. *Nature* **506**, 307-315 (2014).
215 Farrell, U. C. *et al.* The sedimentary geochemistry and paleoenvironments project. *Geobiology* **19**, 545-556 (2021).

Acknowledgements

This study was funded by NSFC (42488201, 42325206), the Chinese Academy of Sciences (XDB0710202, XDA0430202), the IGGCAS Key program (no. IGGCAS-202201). KQX is funded by the Hundred Talents Program of the Chinese Academy of Sciences. BJWM is funded by UKRI (grants NE/S009663/1 and EP/Y008790/1). We thank Pengcheng Ju for his valuable insights. We acknowledge 3 anonymous reviews for constructive comments on the manuscript.

Competing interests

The authors declare no competing interests.

Author contributions

M.Z. wrote the manuscript, with significant input from all authors.

Data availability

All the compiled data files for this study are available in the Supplementary Tables.

Code availability

The code for the diagenetic model is available in the Supplementary Information.